© 2023. Published by The Company of Biologists Ltd | Development (2023) 150, dev200436. doi:10.1242/dev.200436

RESEARCH ARTICLE

Ikaros family proteins redundantly regulate temporal patterning in the developing mouse retina

Awais Javed[1,2,*], Pedro L. Santos-França[1,2], Pierre Mattar[1,‡], Allie Cui[1], Fatima Kassem[1,3] and Michel Cayouette[1,2,3,4,5,§]

ABSTRACT

Temporal identity factors regulate competence of neural progenitors to generate specific cell types in a time-dependent manner, but how they operate remains poorly defined. In the developing mouse retina, the Ikaros zinc-finger transcription factor Ikzf1 regulates production of early-born cell types, except cone photoreceptors. In this study we show that, during early stages of retinal development, another Ikaros family protein, Ikzf4, functions redundantly with Ikzf1 to regulate cone photoreceptor production. Using CUT&RUN and functional assays, we show that Ikzf4 binds and represses genes involved in late-born rod photoreceptor specification, hence favoring cone production. At late stages, when Ikzf1 is no longer expressed in progenitors, we show that Ikzf4 re-localizes to target genes involved in gliogenesis and is required for Müller glia production. We report that Ikzf4 regulates Notch signaling genes and is sufficient to activate the *Hes1* promoter through two Ikzf GGAA-binding motifs, suggesting a mechanism by which Ikzf4 may influence gliogenesis. These results uncover a combinatorial role for Ikaros family members during nervous system development and provide mechanistic insights on how they temporally regulate cell fate output.

KEY WORDS: Retina, Development, Temporal patterning, Photoreceptors, Gliogenesis

INTRODUCTION

The generation of cell diversity in the central nervous system (CNS) is a highly controlled and regulated process. Neural progenitors alter their potential to generate specific neurons and glia using both spatial and temporal patterning cues (Sagner and Briscoe, 2019). In the *Drosophila* nervous system, temporal patterning is regulated by the expression of transcription factors referred to as 'temporal identity' factors, which control the developmental competence of neural progenitor cells, allowing cell-type production to change as development proceeds (Brody and Odenwald, 2000; Cleary and Doe, 2006; Erclik et al., 2017; Grosskortenhaus et al., 2005, 2006; Isshiki et al., 2001; Kambadur et al., 1998; Li et al., 2013; Novotny et al., 2002; Pearson and Doe, 2003). A classic example of temporal patterning in vertebrates is the developing mouse retina, where seven broad cell types are formed in a sequential but overlapping manner from multipotent retinal progenitor cells (RPCs) (Rapaport et al., 2004; Young, 1985a,b). Retinal ganglion cells (RGCs), amacrine cells, cone photoreceptors and horizontal cells are mostly generated during the embryonic period of retinogenesis, whereas rod photoreceptors, bipolar cells and Müller glia are primarily generated during the rodent postnatal period (Carter-Dawson and LaVail, 1979a,b; Rapaport et al., 2004; Turner et al., 1990; Young, 1985a,b).

How exactly RPCs change competence over time to control retinal histogenesis remains poorly understood, although some progress was made in recent years (Davis et al., 2011; Decembrini et al., 2009; Dupacova et al., 2021; Elliott et al., 2008; Georgi and Reh, 2010; Gordon et al., 2013; Iida et al., 2011; Javed et al., 2020; La Torre et al., 2013; Mattar et al., 2015; Yang et al., 2003; Zibetti et al., 2019). Of note, homologs of *Drosophila* temporal identity factors were found to regulate temporal patterning in mouse RPCs (Elliott et al., 2008; Javed et al., 2020; Mattar et al., 2015). Specifically, inactivation of *Ikzf1* (a homolog of *Drosophila hunchback*), a member of the Ikaros family of zinc-finger transcription factors, leads to reduced numbers of early born cell types in the retina, except cone photoreceptors, which remain unchanged (Elliott et al., 2008). Together with data showing that stochastic mechanisms contribute to cell diversification in the developing retina (Gomes et al., 2011; He et al., 2012), this work has led to a model in which temporal identity factors function permissively to bias the probability of generating specific combinations of cell types at different times (Mattar and Cayouette, 2015). Thus, loss of Ikzf1 reduces the chance of generating most early-born cell types, rather than completely blocking their production. However, the mechanisms regulating the timely generation of cones are still unclear. Recently, the homolog of *Drosophila pdm/nub*, *Pou2f1*, was shown to play a part in the temporal regulation of cone photoreceptor production by upregulating Pou2f2, which in turn represses the rod determinant Nrl in photoreceptor precursors, thereby favoring the cone fate (Javed et al., 2020). Intriguingly, Ikzf1 was found to upregulate Pou2f1 expression, but because Ikzf1 knockout retinas have normal numbers of cones (Elliott et al., 2008), these results suggest that unidentified factor(s) might function with Ikzf1 to confer competence in RPCs to generate cones.

Mechanisms regulating the production of late-born cell types also remain incompletely understood. The homolog of *Drosophila castor*, *Casz1*, another zinc-finger transcription factor, confers competence to generate mid/late-born rod and bipolar cells in the mouse retina, while suppressing the production of Müller glia, the latest-born cell type (Mattar et al., 2015). Foxn4 was found to

[1]Cellular Neurobiology Research Unit, Institut de recherches cliniques de Montréal (IRCM), Montreal H2W 1R7, Canada. [2]Molecular Biology Program, Université de Montréal, Montreal H3T 1J4, Canada. [3]Integrated Program in Neuroscience, McGill University, Montreal H3A 0G4, Canada. [4]Department of Medicine, Université de Montréal, Montreal H3T 1J4, Canada. [5]Department of Anatomy and Cell Biology, Division of Experimental Medicine, McGill University, Montreal H3A 0G4, Canada. *Present address: Department of Basic Neurosciences, Centre Medical Universitaire (CMU), Université de Genève, Geneva 1206, Switzerland. ‡Present address: Department of Cell and Molecular Medicine, University of Ottawa, Ottawa K1N 6N5, Canada.

§Author for correspondence (michel.cayouette@ircm.qc.ca)

P.M., 0000-0002-5708-6218; M.C., 0000-0003-4655-9048

Handling Editor: François Guillemot
Received 7 December 2021; Accepted 6 December 2022

Development (2023) 150, dev200436. doi:10.1242/dev.200436

operate downstream of Ikzf1 and upstream of Casz1 to regulate mid-late temporal identity (Liu et al., 2020), but it is not involved in Müller glia production. Instead, the temporal regulation of Müller glia production in the developing mouse retina appears largely regulated by the Nfi family of transcription factors (Clark et al., 2019), which promote expression of glial differentiation genes, even in early-stage RPCs that do not normally generate glia (Lyu et al., 2021 preprint). It remains unclear, however, how exactly Nfi factors are upregulated during late stages of retinogenesis to control glia production. Additionally, Sox9, Vsx2 and Sox2 regulate Müller glia development but, as they are broadly expressed throughout retinal development, it is unclear how their pro-glial activities are temporally gated (Lin et al., 2009; Livne-bar et al., 2006; Poché et al., 2008; Surzenko et al., 2013; Taranova et al., 2006).

There are five members of the Ikaros family of transcription factors in mice, four of which are expressed in the developing retina (Elliott et al., 2008). Aside from Ikzf1, the role of Ikaros family members in the mammalian CNS has not been explored. We therefore wondered whether other Ikaros family members might contribute to regulating RPC competence during mouse retinogenesis. We show here that Ikzf4 is required together with Ikzf1 to control cone production during early stages of retinogenesis. At late stages, we report that Ikzf4 is required for Müller glia production. Using CUT&RUN and transcriptional assays, we show that Ikzf4 binds to cis-regulatory elements of genes involved in repressing the rod photoreceptor fate at early stages, and then switches to bind genes involved in Müller glia production at late stages. Together with previous observations, these results suggest combinatorial roles for Ikzf1 and Ikzf4 during retinogenesis to regulate cell fate in a context- and temporal-dependent manner.

RESULTS

Ikzf4 is expressed in retinal progenitor cells at all stages of retinogenesis

We have previously reported expression of Ikzf4 transcripts in the retina using *in situ* hybridization (Elliott et al., 2008), but the protein expression pattern remained unknown. To fill this knowledge gap, we characterized a commercially available anti-Ikzf4 antibody. First, we electroporated CAG:GFP or CAG:Ikzf4-IRES-GFP vectors in E17 mouse retinas and immunostained retinal sections 2 days later using the Ikzf4 antibody. As expected, we found that the antibody recognizes overexpressed Ikzf4 proteins (Fig. S1A-C′). Second, to ensure that the antibody is specific for Ikzf4, we immunostained retinas isolated from *Ikzf4*$^{+/+}$ and *Ikzf4*$^{-/-}$ (RIKEN Bioresource https://scicrunch.org/resolver/IMSR_RBRC06808) mouse embryos at E12, E15 and P9. We found that Ikzf4 is expressed in virtually all retinal cells at E12 and E15, whereas it is restricted to a few retinal cell subtypes at P9 (Fig. S1D-H). No immunostaining signal was detected in the *Ikzf4*$^{-/-}$ retinas, indicating that the antibody specifically recognizes Ikzf4 (Fig. S1D-H′). We hypothesized that Ikzf4 was expressed in RPCs based on its expression pattern. Accordingly, we found that virtually all proliferating Ki67^{+ve} RPCs also stained for Ikzf4 at embryonic stages (Fig. 1A-C), and many Ki67^{+ve} cells also co-labeled with Ikzf4 at P0 and P2 (Fig. 1D-F), indicating that Ikzf4 is expressed in RPCs throughout development.

We next compared our immunostaining data for Ikzf4 with published scRNA-seq datasets in the developing mouse and human fetal retinas (Clark et al., 2019; Lu et al., 2020). Focusing on the RPC population, we generated UMAP plots by sub-setting the RPC populations at various developmental stages. We found that *Ikzf4*/*IKZF4* mRNA is expressed in both early and late RPCs (Fig. S1I,J), consistent with our immunostaining results. In addition to RPCs and neurogenic progenitors, we found *Ikzf4/IKZF4* expression in differentiated retinal cell type clusters such as rods, amacrine, horizontal and retinal ganglion cells (Fig. S2A,B).

To assess expression of Ikzf4 in mature cells, we used cell-type specific antibodies at P7. We detected expression of Ikzf4 in early-born cell types such as Lim1^{+ve} horizontal cells, Brn3a^{+ve} RGCs, Pax6^{+ve} amacrine cells and S-opsin^{+} cone photoreceptors (Fig. 1G-H‴). We could also detect weak Ikzf4 immunostaining in S-opsin^{-} cells in the ONL, suggesting some expression in rod photoreceptors (Fig. 1H′,H″). These results are consistent with our *Ikzf4*/*IKZF4* expression analysis in scRNA-seq datasets (Clark et al., 2019; Lu et al., 2020) (Fig. S2A,B). Interestingly, we also found Ikzf4 expression in Nfia^{+} and/or Nifb^{+} cells that are either Chx10^{-} or Chx10^{+} (Fig. 1I-I‴), likely representing Müller glia and bipolar cells, respectively. Taken together, these data indicate that Ikzf4 is detected in all mature early-born cell types and in some late-born cell types.

Ikzf4 overexpression in late-stage retinal progenitors represses rod and promotes Müller glia production

To investigate Ikzf4 function in the developing mouse retina, we genetically manipulated late-stage RPCs by misexpressing Ikzf4. We first infected P0 retinal explants with retroviral vectors expressing Venus or Ikzf4-IRES-Venus and analyzed individual clone compositions 14 days later using cell type-specific markers, cell morphology and nuclear layer position, as we did previously (Elliott et al., 2008; Javed et al., 2020). In the Ikzf4-IRES-Venus-infected clones, we found many Venus^{+} cells located in the ONL that stained for Rxrg, a marker of cone photoreceptors in this layer (Fig. 2A-B″), as well as many cells with a Müller glia morphology (Fig. 2C). Quantifications revealed a significant increase in the proportion of Rxrg^{+} cone-like cells and Müller glia in the Venus^{+} clones, at the expense of rods (Fig. 2D). The proportion of one-cell clones was also slightly increased after *Ikzf4* expression (Fig. 2E), suggesting precocious cell cycle exit or cell death. To distinguish between these possibilities, we electroporated CAG:GFP or CAG:Ikzf4-IRES-GFP vectors in P0 retinas. After culturing retinal explants for 2 days, we added EdU for 2 h then fixed and stained the explants for GFP and EdU. We observed a significant decrease in EdU^{+}GFP^{+} cells after expression of Ikzf4 (Fig. 2F-H). As we found no change in the number of cells staining for cleaved caspase 3 (Fig. S3A-C), we conclude that Ikzf4 expression reduces clone size by promoting early cell cycle exit, rather than cell death. Finally, we also found that most one- and two-cell clones in the Ikzf4 condition contain either cone-like cells or Müller glia, whereas control clones contain mostly rods (Fig. S3D,E). Together, these results suggest that Ikzf4 promotes cone-like cells and Müller glia fate at the expense of rods when expressed in late RPCs.

To support the retroviral lineage-tracing results and provide more in-depth analysis of the cell types produced, we electroporated retinas *in vivo* at P0 with either CAG:GFP or CAG:Ikzf4-IRES-GFP and determined the identity of GFP^{+} cells 14 days later using immunostaining for cell type-specific markers. As observed with retroviral vectors, we found an increase in Rxrg^{+}GFP^{+} cells following Ikzf4 electroporation (Fig. 2I-K). Although endogenous cones expressed both Rxrg and S-opsin, as expected, GFP^{+} cells in the Ikzf4 condition expressed Rxrg, but not S-opsin or other mature cone markers such as M-opsin and PNA (Fig. S3F-G‴). The GFP^{+}Rxrg^{+} cells we found in the ONL were not mis-localized retinal ganglion cells (RGCs), which also express Rxrg (Mori et al., 2001), as they did not express markers of RGCs, such as Brn3a or Brn3b (Fig. S3H-I‴). Instead, Ikzf4-expressing GFP^{+} cells in the

Development (2023) 150, dev200436. doi:10.1242/dev.200436

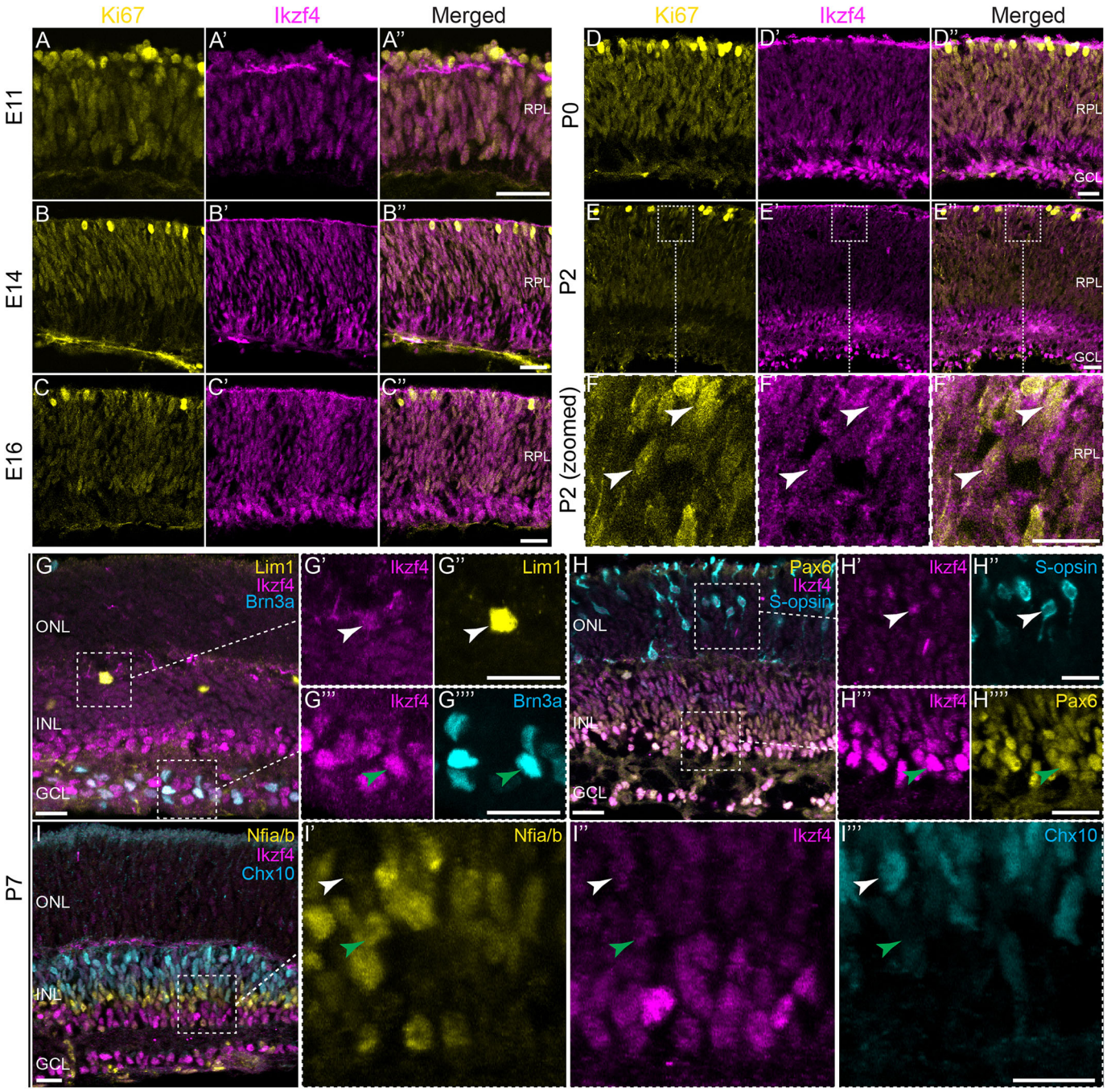

Fig. 1. Ikzf4 is expressed during early and late stages of retinogenesis. (A-E″) Co-immunostaining for Ki67 (yellow) and Ikzf4 (magenta) at various stages of mouse retinal development. (F-F″) Zoomed-in images of E-E″; arrowheads indicate co-expression of Ki67 (yellow) and Ikzf4 (magenta) in some cells. (G-I‴) Zoomed-out (G,H,I) and zoomed-in (G′-G‴,H′-H‴,I′-I‴) examples of P7 mouse retinas co-immunostained for Ikzf4 (G′,G‴,H′,H‴,I″), Lim1 (G″), Brn3a (G‴), S-opsin (H″), Pax6 (H‴), Nfia/b (I′) and Chx10 (I‴). White arrowheads indicate Ikzf4^{+}Lim1^{+} (G′,G″), Ikzf4^{+}S-opsin^{+} (H′,H″) and Nfia/b^{+}Ikzf4^{+}Chx10^{+} (I′-I‴) cells. Green arrowheads indicate Ikzf4^{+}Brn3a^{+} (G‴,G⁗), Pax6^{+}Ikzf4^{+}(H‴,H⁗) and Nfia/b^{+}Ikzf4^{+ve}Chx10^{-} (I′-I‴). Zoomed in regions are indicated with dashed squares. RPL, retinal progenitor layer; ONL, outer nuclear layer; INL, inner nuclear layer; GCL, ganglion cell layer. Scale bars: 20 µm in A-E″; 10 µm in F-I‴.

ONL co-labeled with Crx/Otx2, which specifically labels photoreceptor cells in this layer and bipolar cells in the INL at the equivalent age of P14 (Fig. S3J-K″). Thus, consistent with our observations in explants infected with retroviral vectors, expression of Ikzf4 in postnatal RPCs induces the generation of cone-like cells. Also consistent with our retroviral experiments in explants, we observed GFP^{+}Sox2^{+}, GFP^{+}Hes1^{+}Chx10^{-} and GFP^{+}Lhx2^{+}Nfia/b^{+} Müller glia after electroporation of Ikzf4 in P0 RPCs *in vivo* and *ex vivo* (Fig. S3L-O″). These cells had typical Müller glia morphology with apical and basal processes extending through the entire retina, indicating that expression of Ikzf4 in P0 RPCs also promotes the glial fate.

As photoreceptor precursors normally give rise to rods at postnatal stages, we postulated that the immature cones generated might be the result of Ikzf4 inhibiting rod production. Consistent with this hypothesis, we observed a reduction in transcript levels of *Nrl* and

Development (2023) 150, dev200436. doi:10.1242/dev.200436

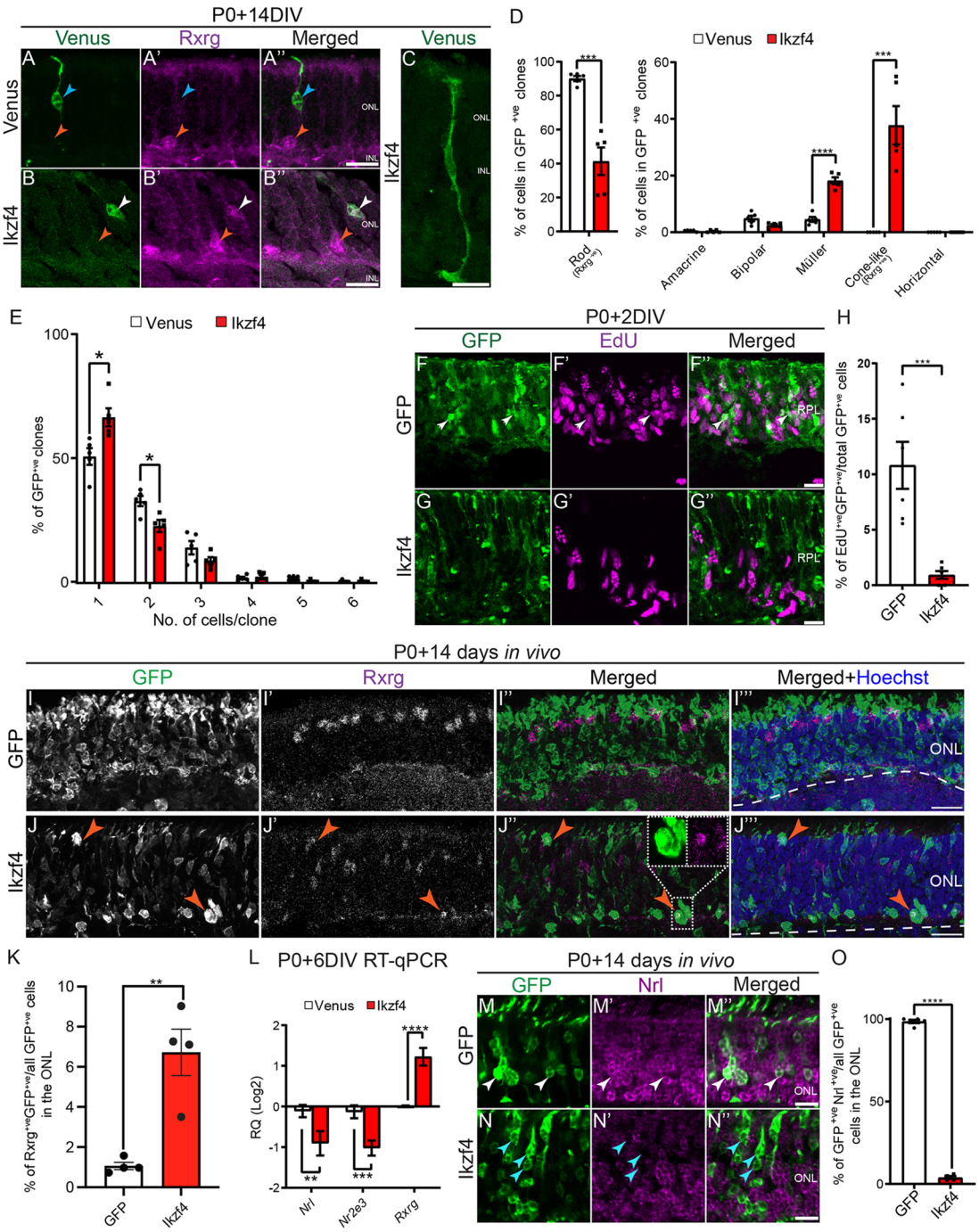

Fig. 2. Ikzf4 promotes Müller glia and cone-like cell generation, and inhibits rod cell fate from late-stage RPCs. (A-B″) Examples of clones obtained after infection with retroviral vectors expressing Venus (A) and Ikzf4-IRES-Venus (B) co-immunostained with Rxrg (A′,B′), a cone marker. (C) Example of Müller glia generated by Ikzf4 retroviral infection. (D,E) Retroviral lineage analysis of Venus control (469 clones counted) and Ikzf4-IRES-Venus (388 clones counted) overexpression in late-stage retinas. (D) Quantifications for cell type analysis was based on morphology and laminar positioning of the cell bodies in the retina (Venus, *n*=5; Ikzf4, *n*=5). Cones (Rxrg$^+$) and rods (Rxrg$^-$) were counted in the ONL based on Rxrg expression. (E) Quantifications of the number of cells per clone for the data presented in D. (F-G″) Examples of P0 retinal explants electroporated with either GFP (F-F″) or Ikzf4 (G-G″), with 30 µM EdU added to the culture medium 2 days later. Retinal explants were immunostained with EdU after fixation. White arrowheads indicate GFP$^+$EdU$^+$ cells. (H) Quantification of the number of EdU$^+$GFP$^+$ cells [GFP (593 cells counted), *n*=6; Ikzf4 (676 cells counted), *n*=6]. (I-J‴) Examples of retinas electroporated *in vivo* with either GFP (I,I″,I‴) or Ikzf4 (J,J″,J‴) and immunostained for Rxrg (I′,J′) 14 days after electroporation. Orange arrowheads indicate GFP$^+$Rxrg$^+$ cells. Area above the dashed line represents the outer nuclear layer. (K) Quantification of the number of GFP$^+$Rxrg$^+$ cells [GFP (736 cells counted), *n*=4; Ikzf4 (642 cells counted), *n*=4]. (L) RT-qPCR analysis of *Nrl*, *Nr2e3* and *Rxrg* expression from sorted GFP$^+$ cells 6 days after electroporation of P0 retinal explants with either GFP (*n*=5) or Ikzf4 (*n*=5). (M-N″) Examples of retinas electroporated *in vivo* at P0 with either GFP (M-M″) or Ikzf4-IRES-GFP (N-N″) and immunostained for Nrl (M′,M″,N′,N″) 14 days later. White arrowheads indicate GFP$^+$Nrl$^+$ cells; cyan arrowheads indicate GFP$^+$Nrl$^-$ cells. (N) Quantification of the number of GFP$^+$Nrl$^+$ cells (GFP, *n*=5; Ikzf4, *n*=4). **P*<0.05, ***P*<0.01, ****P*<0.001, *****P*<0.0001 [two-tailed unpaired *t*-test (D,E,H,K,O), Mann–Whitney test (L)]. RPL, retinal progenitor layer; ONL, outer nuclear layer; INL, inner nuclear layer; RQ, relative quantitation. Scale bars: 10 µm.

Development (2023) 150, dev200436. doi:10.1242/dev.200436

Nr2e3, two rod-specific genes, and an increase in *Rxrg* expression in the GFP$^+$ cell population 6 days after electroporation of CAG:Ikzf4-IRES-GFP in P0 retinal explants (Fig. 2L). The number of GFP$^+$ cells in the ONL that stain for Nrl and Nr2e3 was also reduced after Ikzf4 expression (Fig. 2M-O, Fig. S3P-Q″). Thus, we conclude that expression of Ikzf4 in late-stage RPCs promotes glia and represses the rod photoreceptor fate, which lead to photoreceptor precursors turning on Rxrg expression. We postulate that the lack of a transcriptional network promoting cone differentiation at P0 prevents the full maturation of Ikzf4-induced cone-like cells.

Ikzf4 is required for Müller glia development

Based on the above results, we hypothesized that Ikzf4 may be required for cone and Müller glia development. We therefore analyzed retinas from *Ikzf4*$^{+/+}$, *Ikzf4*$^{+/-}$ and *Ikzf4*$^{-/-}$ mice, and quantified the various retinal cell types using specific markers at P10, a stage when cell genesis is largely complete. Although we found no change in the number of RGCs (Brn3a$^+$), amacrine cells (Pax6$^+$), horizontal cells (Lim1$^+$) or bipolar cells (Otx2$^+$), we observed a reduction in Sox2$^+$ and Lhx2$^+$ Müller cells in the INL of *Ikzf4*$^{-/-}$ retinas compared with *Ikzf4*$^{+/+}$ and *Ikzf4*$^{+/-}$ retinas (Fig. 3A-C). Unexpectedly, we found no difference in the number of Rxrg$^+$ cells in the ONL in *Ikzf4*$^{-/-}$ retinas compared with control *Ikzf4*$^{+/+}$ (Fig. 3C). These results indicate that Ikzf4 is required for Müller glia development, but not for cone photoreceptors.

Ikzf4 functions redundantly with Ikzf1 to partially control cone photoreceptor development

We have previously shown that inactivation of Ikzf1 decreases early-born cell type production, with the exception of cone photoreceptors, which are unaltered in Ikzf1 KO mice (Elliott et al., 2008). As Ikzf1 and Ikzf4 are expressed in the same cells as early as E11 (Fig. S4A-D), we wondered whether Ikzf1 and Ikzf4 might genetically interact to regulate cone development. To test this idea, we generated Ikzf1 and Ikzf4 double knockout mice. Interestingly, when both alleles of *Ikzf1* were knocked out together with one or two alleles of *Ikzf4* (*Ikzf1*$^{-/-}$;*Ikzf4*$^{+/-}$ and *Ikzf1*$^{-/-}$;*Ikzf4*$^{-/-}$), embryos were paler and exhibited reduced liver size compared with *Ikzf1*$^{+/-}$;*Ikzf4*$^{-/-}$ and *Ikzf1*$^{+/-}$;*Ikzf4*$^{+/-}$ embryos (Fig. S4E-H). Moreover, we found that *Ikzf1*$^{-/-}$;*Ikzf4*$^{+/-}$ and *Ikzf1*$^{-/-}$;*Ikzf4*$^{-/-}$ mice die at early perinatal stages, usually before P2, whereas single *Ikzf1*$^{-/-}$ or *Ikzf4*$^{-/-}$ mice are viable, showing functional redundancy for survival. Therefore, we had to focus our analysis of the retina at embryonic stages.

We first quantified cone numbers using Rxrg immunostaining at E15, when cone genesis is at its peak. Although we found no difference in cone photoreceptor numbers between most genotypes analyzed, we found a significant reduction in cone numbers in *Ikzf1*$^{-/-}$;*Ikzf4*$^{-/-}$ double knockout animals (Fig. 3D-F), indicating an epistatic relationship between Ikzf1 and Ikzf4 to control cone photoreceptor development, at least partially. We also investigated whether Ikzf4 might function with Ikzf1 to regulate production of other early-born cell types, which are only mildly decreased in *Ikzf1* KO retinas (Elliott et al., 2008). As the expression of specific amacrine and horizontal cell markers generally starts at postnatal stages (Clark et al., 2019), when double knockout animals are lethal, we focused our attention on RGC production, as Brn3b is robustly expressed at E15.5 (Xiang, 1998). We found that the number of RGCs is reduced in *Ikzf1*$^{-/-}$;*Ikzf4*$^{+/-}$ (Fig. 3G), consistent with our previously-published data (Elliott et al., 2008), but this was not enhanced in *Ikzf1*$^{-/-}$;*Ikzf4*$^{-/-}$ double knockout animals. Thus, unlike our observations for cones, Ikzf4 does not act redundantly with Ikzf1 to regulate RGC development.

Ikzf1 regulates genes involved in early-born cell type production

We have previously reported that expression of Ikzf1 in late RPCs is sufficient to confer competence to generate early-born horizontal, amacrine and retinal ganglion cells (Elliott et al., 2008). To explore how Ikzf1 might temporally reprogram late-stage RPCs, we misexpressed Ikzf1 in P0 retinas, and carried out CUT&RUN and RNA-sequencing (Fig. S5A). We first curated the top differentially expressed genes by comparing the RNA-seq datasets from the CAG-GFP and CAG-Ikzf1-transfected RPCs using DESeq2 (Fig. S5A, Table S1). We performed gene ontology (GO) enrichment using GONet to find the top biological processes affected by Ikzf1 misexpression (Pomaznoy et al., 2018). In the upregulated list, we found many genes associated with retinal ganglion cells and amacrine cell development, such as *Bhlhe22*, *Tfap2b*, *Nr4a2* and *Pax6* under the GO biological process 'nervous system development', as predicted given that Ikzf1 promotes these early-born cell fates (Fig. S5B, Table S2) (Elliott et al., 2008). Conversely, in the downregulated list, we found many genes associated with bipolar and Müller glia development such as *Hes1*, *Irx3*, *Notch3*, *Rbpj*, *Sox2* and *Sox9* under the GO biological process 'regulation of neuron differentiation' (Fig. S5B, Table S3). We also found the late temporal factor *Casz1* in the same GO biological process, consistent with our previously published results that Ikzf1 represses *Casz1* (Mattar et al., 2015). We next assessed the CUT&RUN feature distribution using ChIPSeeker to annotate the MACS2 called peaks (Yu et al., 2015), and found that Ikzf1 binding is mostly observed away from the promoters in intergenic and intronic regions (Fig. S5C), as previously reported in B cells (Schwickert et al., 2014). Using Hypergeometric Optimization of Motif EnRichment (HOMER) to discover transcription factor motifs (Heinz et al., 2010), we found the canonical 'GGAA' Ikzf-binding motif (Molnár and Georgopoulos, 1994) or the complementary sequence in the dataset (Fig. S5D), as predicted. These results suggest that Ikzf1 binds to GGAA motifs in distal and intronic cis regulatory elements (CRE). To narrow down the list of potential target genes, we next compared the significantly altered transcripts in Ikzf1 misexpression RNA-seq with that of bound regions in Ikzf1 CUT&RUN using Genomic Regions Enrichment of Annotations Tool (GREAT) (Table S4) (McLean et al., 2010). We found a total of around 1000 upregulated and downregulated transcripts that are bound by Ikzf1 (Fig. S5E, Table S5). Out of these, retinal ganglion cell and amacrine cell development genes were enriched in the upregulated category, such as *Bhlhe22*, *Nr4a2* and *Tfap2b*, whereas bipolar cell and Müller glia development genes, such as *Casz1*, *Hes1*, *Irx3*, *Irx5*, *Irx6*, *Nfib*, *Rbpj* and *Sox2*, were enriched in the downregulated category (Fig. S5F,G, Table S4). These results are consistent with Ikzf1 functioning as an early temporal identity factor through the positive and negative regulation of multiple genes involved in early- and late-born cell type production, respectively.

Ikzf4 binds and regulates genes involved in cone development during early stages of development

To provide molecular insights into Ikzf4 function in retinal development, we first carried out CUT&RUN on E14 and P0 retinal extracts using a validated anti-Ikzf4 antibody (S1A-H′). As the expression of Ikzf4 in E14 and P0 mouse retinas is mostly restricted to RPCs, with only a small number of differentiated cells also expressing Ikzf4, we postulated that this experiment would give a reliable read-out of Ikzf4-binding targets in RPCs. Using MACS2 peak calling on the CUT&RUN datasets, we found 2472 Ikzf4 peaks at E14 and 2130

Development (2023) 150, dev200436. doi:10.1242/dev.200436

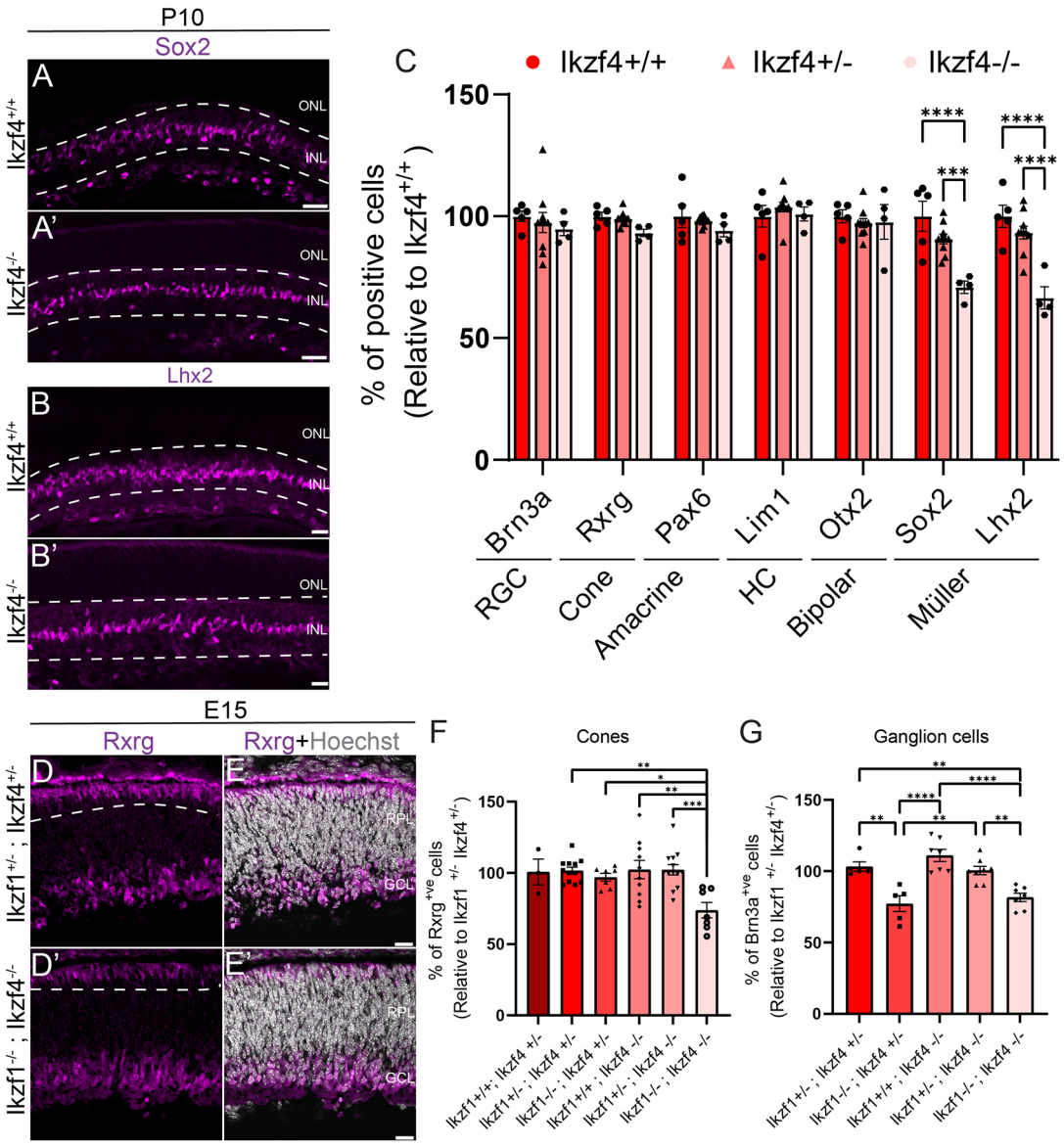

Fig. 3. Combinatorial requirement for Ikzf1 and Ikzf4 in the production of cones during early retinogenesis and Müller glia during late retinogenesis. (A-C) Examples of Sox2 (A,A′) and Lhx2 (B,B′) immunostaining in either *Ikzf4*$^{+/+}$ (A,B) or *Ikzf4*$^{-/-}$ (A′,B′) mouse retinas at P10. (C) Quantification of various retinal cell types using specific markers in either *Ikzf4*$^{+/+}$ (*n*=7), *Ikzf4*$^{+/-}$ (*n*=13) or *Ikzf4*$^{-/-}$ (*n*=7) mouse retinas. (D-E′) Examples of Rxrg (D,D′) immunostaining in either *Ikzf1*$^{+/-}$*Ikzf4*$^{+/-}$ (D,E) or *Ikzf1*$^{-/-}$*Ikzf4*$^{-/-}$ (D′,E′) mouse retinas at E15. (F) Quantification of Rxrg^{+} cells in *Ikzf1*$^{+/+}$*Ikzf4*$^{+/-}$ (*n*=3), *Ikzf1*$^{+/-}$*Ikzf4*$^{+/-}$ (*n*=12), *Ikzf1*$^{-/-}$*Ikzf4*$^{+/-}$ (*n*=7), *Ikzf1*$^{+/+}$*Ikzf4*$^{-/-}$ (*n*=10), *Ikzf1*$^{+/-}$*Ikzf4*$^{+/-}$ (*n*=13) or *Ikzf1*$^{-/-}$*Ikzf4*$^{-/-}$ (*n*=7) mouse retinas. (G) Quantifications of Brn3a^{+} cells in either *Ikzf1*$^{+/-}$*Ikzf4*$^{+/-}$ (*n*=5), *Ikzf1*$^{-/-}$*Ikzf4*$^{+/-}$ (*n*=5), *Ikzf1*$^{+/+}$*Ikzf4*$^{-/-}$ (*n*=7), *Ikzf1*$^{+/-}$*Ikzf4*$^{+/-}$ (*n*=8) or *Ikzf1*$^{-/-}$*Ikzf4*$^{-/-}$ (*n*=7) mouse retinas. **P*<0.05, ***P*<0.01, ****P*<0.001, *****P*<0.0001 (one-way ANOVA with Tukey's correction). RPL, retinal progenitor layer; ONL, outer nuclear layer; INL, inner nuclear layer. GCL, ganglion cell layer. Scale bars: 10 µm.

peaks at P0 (Fig. S6A). When we intersected the peaks between the Ikzf1 at P0 and Ikzf4 E14 and P0 datasets using bedtools (Quinlan and Hall, 2010), we found only a few overlapping peaks (Fig. S6A), suggesting that Ikzf1 and Ikzf4 do not bind to the same cis-regulatory elements (CREs) in RPCs. Using ChIPSeeker and HOMER (Heinz et al., 2010; Yu et al., 2015), we found that Ikzf4 primarily binds to the 'GGAA' motif or the complementary sequence in promoters at both E14 and P0 (Fig. S6B,C).

Next, we carried out GO classification using GREAT and annotated the top GO biological processes at E14 (Table S6) (McLean et al., 2010). We found that 'Positive regulation of chromatin organization' was one of the top biological processes (Fig. 4A). Among the list of bound genes associated with this GO term, we found the DNA methyltransferase *Dnmt1*, which has previously been shown to regulate photoreceptor differentiation (Fig. 4A) (Rhee et al., 2012), suggesting a role for Ikzf4 in the regulation of chromatin organizers during early retinogenesis. We next focused our analysis on known regulators of cone or rod cell fate. We found that Ikzf4 binds to many genes involved in suppressing the rod fate and promoting the cone fate, such as *Sall3*, *Thrb*, *Onecut1*, *Onecut2* and *Pou2f2* (de Melo et al., 2011; Emerson et al., 2013; Javed et al., 2020; Jean-Charles et al., 2018; Ng et al., 2001; Sapkota et al., 2014) (Fig. 4B).

Of particular interest to us in the E14 Ikzf4 CUT&RUN data was the peak observed in a region of open chromatin 47 kb upstream of the *Pou2f2* promoter that scored as a significant *Pou2f2*-associated

Development (2023) 150, dev200436. doi:10.1242/dev.200436

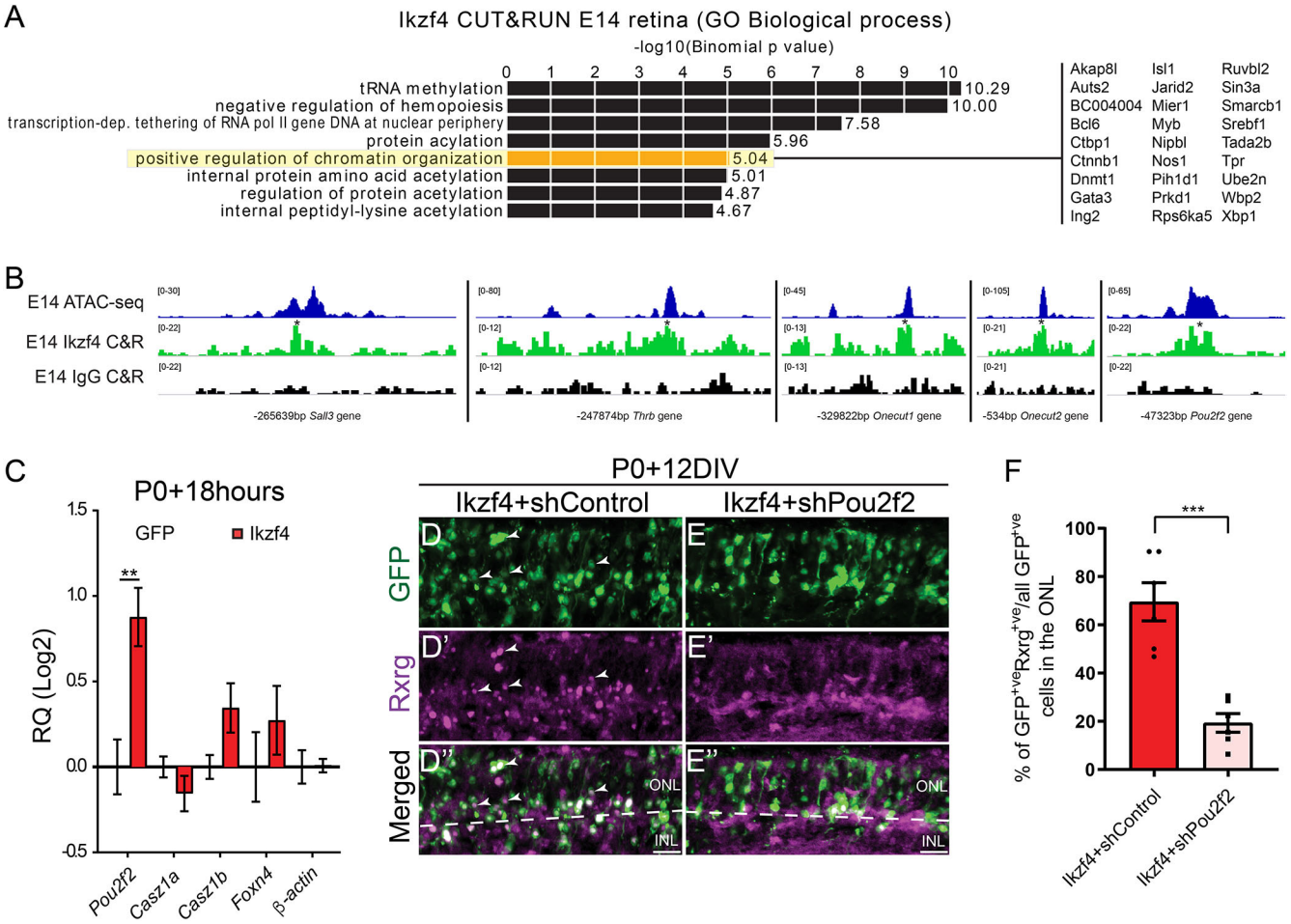

Fig. 4. Ikzf4 binds to target genes involved in rod fate suppression. (A) GREAT analysis on Ikzf4 CUT&RUN peaks at E14. Gene ontology classification of the genes in proximity of Ikzf4-binding peaks. The 'positive regulation of chromatin organization' GO term is highlighted and genes in this list are displayed on the right. (B) Genomic tracks of ATAC-seq at E14 in blue (Aldiri et al., 2017), Ikzf4 CUT&RUN peaks at E14 in green and IgG control CUT&RUN at E14 in black at genomic regions associated with the cone genes *Sall3*, *Thrb*, *Onecut1*, *Onecut2* and *Pou2f2*. Asterisks indicate MACS2-called peaks. (C) RT-qPCR analysis of *Pou2f2*, *Casz1a*, *Casz1b*, *Foxn4* or β-actin from sorted GFP$^+$ cells 18 h after electroporation of P0 retinal explants with either GFP (n=5) or Ikzf4 (n=5).**P<0.01 (Mann–Whitney test). (D-E″) Examples of retinal explants electroporated at P0 with Ikzf4-IRES-GFP and either shControl (D-D″) or shPou2f2 (E-E″), and immunostained for Rxrg (D′,E′). White arrowheads indicate GFP$^+$Rxrg$^+$ cells in the ONL. (F) Quantification of GFP$^+$Rxrg$^+$ cells in the ONL (Ikzf4+shControl, n=6; Ikzf4+shPou2f2, n=6). ***P<0.001 (two-tailed unpaired t-test). RQ, relative quantitation; ONL, outer nuclear layer; INL, inner nuclear layer. Scale bars: 10 µm.

peak using GREAT (Fig. 4B). Indeed, we have previously reported that *Pou2f2* represses the rod-promoting transcription factor *Nrl* to favor cone development. Along with our results showing that Ikzf4 misexpression promotes cone-like cell production and that Ikzf4 is redundantly required with Ikzf1 to promote the cone fate, we hypothesized that Ikzf4 might regulate *Pou2f2* expression to induce cone production. To explore this possibility, we electroporated P0 retinas with either CAG:GFP or CAG:Ikzf4-IRES-GFP, and sorted GFP$^+$ cells 18 h later for RT-qPCR. We found that Ikzf4 upregulates transcript levels of *Pou2f2*, whereas there is no change in the expression of temporal identity factors such as *Casz1a*, *Casz1b* and *Foxn4*, which are regulated by Ikzf1 (Fig. 4C) (Liu et al., 2020; Mattar et al., 2015). These results suggest that Ikzf4 promotes cone development, at least in part, by binding and upregulating *Pou2f2* gene expression. Consistently, we found that the number of GFP$^+$Rxrg$^+$ cells in the ONL was significantly reduced when Pou2f2 was knocked down concomitantly with Ikzf4 expression (Fig. 4D-F), indicating that *Ikzf4* requires *Pou2f2* to promote cone development.

Ikzf4 binds and upregulates genes involved in Müller glia production at late stages of development

To gain insights into how Ikzf4 might promote Müller glia development, we classified GO terms using GREAT and annotated the top biological processes from the P0 CUT&RUN data (Table S7) (McLean et al., 2010). Among these, we found an enrichment in Notch signaling-related GO terms (Fig. 5A), containing Notch signaling genes such as *Rbpj*, *Notch*, *Hes1* and *Hes5*, which were previously reported to promote the Müller glia fate (Furukawa et al., 2000; Hojo et al., 2000; Nelson et al., 2011; Zheng et al., 2009). Next, we assessed genes enriched in the Müller glia cluster in P14 scRNA-seq data (Clark et al., 2019). Remarkably, we found Ikzf4-binding peaks in all the top eight genes enriched in the Müller glia cluster, such as *Nlgn1*, *p27kip1* (*Cdkn1b*), *Tuba1b*, *Trpm3*, *Sorcs1*, *Notch1*, *Slc1a3* and *Vim* (Fig. S7A). However, as late RPCs and Müller glia have similar transcriptomes (Blackshaw et al., 2004; Roesch et al., 2008), these genes are also expressed in RPCs, complicating the interpretation of these results. Therefore, we focused our analysis on genes that are required for Müller glia

Development (2023) 150, dev200436. doi:10.1242/dev.200436

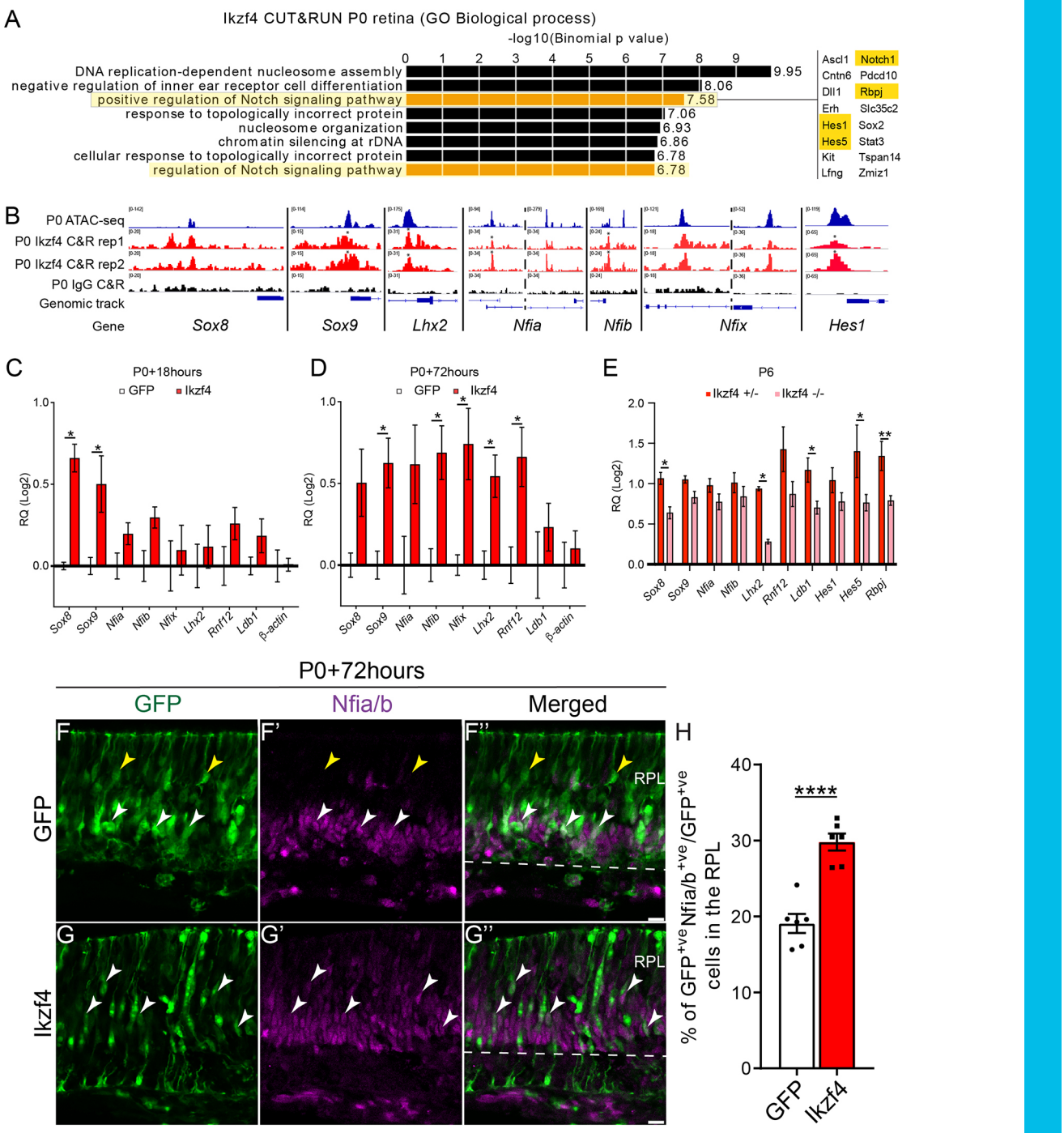

Fig. 5. Ikzf4 binds and regulates expression of Müller specification genes. (A) GREAT analysis on Ikzf4 CUT&RUN peaks at P0. Gene ontology classification of the genes in proximity of Ikzf4-binding peaks. GO terms and associated Notch signaling genes in the list are highlighted and displayed on the right. (B) Genomic peaks of P0 ATAC-seq (Aldiri et al., 2017), P0 Ikzf4 CUT&RUN replicate 1, P0 Ikzf4 CUT&RUN replicate 2 and P0 IgG CUT&RUN at genomic tracks of *Sox8*, *Sox9*, *Lhx2*, Nfi family members and *Hes1*. Asterisks indicate peaks called by MACS2. (C,D) RT-qPCR analysis of Müller specification gene expression from sorted GFP$^+$ cells either 18 h (C) or 72 h (D) after electroporation of P0 retinas with either GFP (n=5) or Ikzf4-IRES-GFP (n=5). (E) RT-qPCR analysis of Müller specification gene expression from P6 retinal mRNA extracts of either *Ikzf4*$^{+/-}$ or *Ikzf4*$^{-/-}$ mice. (F-G″) GFP or Ikzf4-IRES-GFP electroporated retinas *in vitro* at P0 and immunostained for Nfia and/or Nfib 72 h later. (H) Quantification of GFP$^+$Nfia$^+$Nfib$^+$ cells 72 h after electroporation in P0 retinas (GFP, n=6; Ikzf4, n=6). *P<0.05, **P<0.01, ****P<0.0001 [Mann–Whitney test (C-E) or two-tailed unpaired t-test (H)]. RPL, retinal progenitor layer; RQ, relative quantitation. Scale bars: 10 µm in F-G″.

development. We found Ikzf4-binding signal at genomic regions around *Sox8*, *Sox9*, *Lhx2*, *Hes1*, *Nfia*, *Nfib* and *Nfix* gene bodies, some of which were called as peaks by MACS2 (Fig. 5B) (Clark et al., 2019; de Melo et al., 2018, 2016; Muto et al., 2009; Poché et al., 2008; Zibetti et al., 2019). In contrast, we did not find Ikzf4 binding at other intronic open chromatin regions in gene bodies of *Nfib*, *Nfix* and *Nrl*, which are highly expressed at P0, showing the specificity of the identified Ikzf4-binding sites (Fig. S7B).

Next, we performed transcription factor occupancy prediction by investigation of ATAC-seq signal (TOBIAS) on open chromatin

Development (2023) 150, dev200436. doi:10.1242/dev.200436

regions from previously-published datasets (Aldiri et al., 2017) that were bound by Ikzf4 at E14 and P0, to assess motif footprints of transcription factors that could be binding to the same regions as part of a gene regulatory network (Bentsen et al., 2020). We found that, out of the 849 motifs analyzed from the JASPAR database (Fornes et al., 2020), motifs of transcription factors associated with Müller glia differentiation, such as Lhx family, Sox family and Nfib were differentially enriched in P0 open chromatin regions with Ikzf4 binding compared with E14 (Table S8, Fig. S7C,D). We also found that, in the P0 retina, Ikzf4 binds to open chromatin regions that are active or poised enhancers, as suggested by the enrichment of H3K27ac and H3K4me3 histone marks, respectively (Creyghton et al., 2010; Orford et al., 2008), and depletion of the H3K27me3 histone mark (Aldiri et al., 2017; Cao et al., 2002) (Fig. S7E). Therefore, these data suggest that Ikzf4 binds to CREs that are important for Müller glia differentiation at late stages of retinal development.

We then assessed whether Ikzf4 regulates transcripts of genes involved in Müller glia development by electroporating P0 retinas with either CAG:GFP or CAG:Ikzf4-IRES-GFP, and carried out RT-qPCR on sorted GFP$^+$ cells 18 and 72 h later. We found that Ikzf4 promotes expression of *Sox8* and *Sox9* 18 h post-electroporation. Although we found no change in *Lhx2*, *Rnf12*, *Nfia*, *Nfib*, *Nfix* or *Ldb1* at 18 h (Fig. 5C), their expression was increased 72 h after electroporation (Fig. 5D). Conversely, we found a reduction in many Müller glia specification genes in P6 Ikzf4$^{-/-}$ retinas compared with Ikzf4$^{+/-}$, including *Sox8*, *Lhx2*, *Hes5* and *Rbpj* (Fig. 5E). As the Nfi family of proteins are crucial to confer RPC competence to generate Müller glia, we next validated the increase in mRNA levels of *Nfib* by electroporating P0 retinal explants and stained sections for Nfia and Nfib 72 h later. As predicted, we found a significant increase in the number of GFP$^+$ cells stained for Nfia and Nfib after Ikzf4 overexpression (Fig. 5F-H). These results suggest that Ikzf4 is sufficient to induce Müller glia production by binding to and upregulating genes involved in glial cell specification, including Notch signaling genes and Nfi temporal identity factors.

Ikzf4 upregulates *Hes1* by binding to a consensus Ikaros-binding site in the promoter in a Notch-dependent manner

It has previously been shown that *Hes1* expression oscillates during progenitor proliferation (Shimojo et al., 2008). Interestingly, *Hes1* expression decreases when the RPCs exit the cell cycle and is repressed in cells fated to become neurons, whereas it is maintained in cells fated to become glia (Furukawa et al., 2000; Imayoshi et al., 2013). As our CUT&RUN data indicate that *Hes1* locus is significantly bound by Ikzf4 (Fig. 5B), we postulated that Ikzf4 might regulate Müller glia production at least partially by regulating Hes1, and perhaps also the other hairy and enhancer-of-split homolog Hes5. To study the dynamics of Ikzf4 binding at the *Hes1* and *Hes5* promoter, we co-electroporated reporter constructs pHes1-dsRed or pHes5-dsRed together with either CAG:GFP or CAG:Ikzf4-IRES-GFP in P0 retinas. We tracked the electroporation patches over time to assess the dynamics of dsRed expression, which reports activity of the promoters. We observed that Ikzf4 promotes the activity of the *Hes1* promoter compared with the control GFP at 48 and 72 h (Fig. S8A-D″). Even 6 days after electroporation, Ikzf4-electroporated retinas maintained high expression of dsRed, whereas expression of dsRed was reduced in the control GFP condition (Fig. S8E-F″). In contrast, we did not observe similar dynamics in dsRed expression for the *Hes5* promoter at 48 h or 6 days after Ikzf4 electroporation compared with the GFP control (Fig. S8G-J″). Of note, Ikzf4-mediated upregulation of the *Hes1* promoter activity appears to be specific to retinal cells, as Ikzf4 had no effect on pHes1-dsRed activity in HEK293 cells (Fig. S8K-L″). We next assessed whether the increase in *Hes1* promoter activity leads to an increase in Hes1 protein expression. To test this, we electroporated P0 retinas with either CAG:GFP or CAG:Ikzf4-IRES-GFP and analyzed the number of GFP$^+$ cells staining for Hes1 in retinal sections 44 h later. As predicted, we observed an increase in the number of GFP$^+$Hes1$^+$ cells after Ikzf4 expression (Fig. 6A-C). Together, these results indicate that Ikzf4 activates the *Hes1* promoter, which leads to elevation of Hes1 protein expression.

We then sought to identify the Ikzf4-binding sites required for the regulation of *Hes1*. When we analyzed the *Hes1* promoter region containing the Ikzf4 peaks, we found three 'GGAA' Ikzf-binding motifs (Fig. 6D). To study the functional requirement of these motifs, we mutated each one and assessed how this affected the ability of Ikzf4 to regulate the activity of the Hes1 promoter. We co-electroporated CAG:GFP or CAG:Ikzf4-IRES-GFP with either the wild-type or mutated *Hes1* promoter constructs (Fig. 6E). When we mutated binding sites 1 (mut1), 2 (mut2) or 3 (mut3) and electroporated with CAG:GFP, we observed a reduction in dsRed signal compared with the wild-type construct (Fig. 6F-Q), confirming the importance of these sites for the activity of the *Hes1* promoter. However, co-expression of Ikzf4 was sufficient to promote dsRed expression, albeit less so for mut2 (Fig. 6F′-Q′). This suggests that none of these sites alone is required for Ikzf4 binding and activation of the *Hes1* promoter (Fig. 6F-Q′). Interestingly, however, we found that, when we mutated sites 2 and 3 together (mut2+mut3), Ikzf4 was no longer able to activate the *Hes1* promoter (Fig. 6R-T′). Taken together, these results show that Ikzf4 binds at two 'GGAA' sites that are required for the sustained expression of Hes1 in post-mitotic cells.

As Ikzf4 also bound regions associated with other Notch signaling genes, we finally wondered whether the regulation of *Hes1* promoter activity is dependent on Notch signaling. To test this, we electroporated P0 retinas with vectors expressing either GFP or Ikzf4-IRES-GFP, cultured the retinal explants with either DMSO as a control or the Notch signaling inhibitor DAPT, and fixed the explants 6 days later to assess dsRed expression. We found that Ikzf4 overexpression increases the number of dsRed$^+$GFP$^+$ cells in the DMSO condition, whereas this effect is abrogated with the addition of DAPT (Fig. 6U-X), suggesting that Ikzf4 regulates *Hes1* promoter activity in a Notch signaling-dependent manner.

DISCUSSION

Neural diversity in the CNS is generated by a combination of spatial and temporal factors working in concert to establish the vast repertoire of neurons and glia. Although factors regulating fate decisions upon cell cycle exit have been extensively studied, much less is known about how neural progenitors alter their developmental output over time. In this study, we show that Ikzf4 functions epistatically with the previously identified early temporal identity factor Ikzf1 to control the production of early-born cone photoreceptors. We also show that Ikzf4 is required for Müller glia production at late stages of retinogenesis. Mechanistically, we report that, during early stages of development, Ikzf4 generally binds and regulates genes involved in repressing the rod cell fate, including *Pou2f2*, thereby favoring cone production. At late stages, Ikzf4 binds to genes involved in Müller glia development, including *Sox8*, *Sox9*, *Lhx2*, *Nfi* and the Notch signaling effector *Hes1*. Ikzf4 is sufficient to induce sustained expression of *Hes1* during glia

Development (2023) 150, dev200436. doi:10.1242/dev.200436

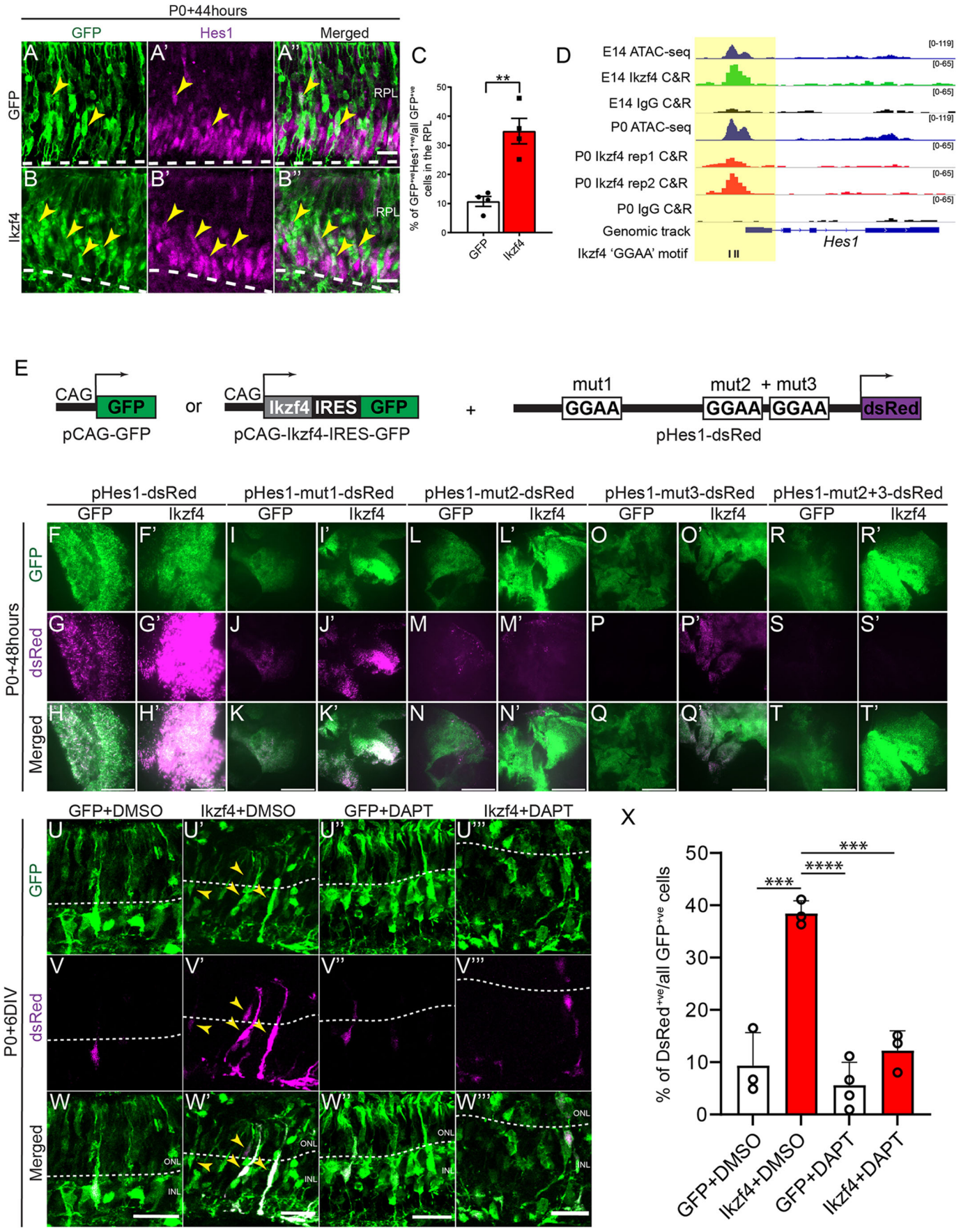

Fig. 6. See next page for legend.

Development (2023) 150, dev200436. doi:10.1242/dev.200436

Fig. 6. Ikzf4 binds to the Hes1 promoter and upregulates Hes1 expression. (A-B″) Examples of GFP (A-A″) or Ikzf4-IRES-GFP- (B-B″) electroporated P0 retinas immunostained for Hes1 44 h later. Yellow arrowheads indicate GFP$^+$Hes1$^+$ cells in the RPL. Area above the dashed lines indicates the RPL. (C) Quantification of GFP$^+$Hes1$^+$ cells in the RPL at P0+44 h after electroporation (GFP, *n*=4; Ikzf4, *n*=4). (D) Genomic peaks of E14 or P0 ATAC-seq (blue) (Aldiri et al., 2017), E14 Ikzf4 CUT&RUN (green), E14 and P0 IgG CUT&RUN (black) and P0 Ikzf4 CUT&RUN replicates 1 and 2 (red) at the Hes1 promoter. Ikzf4 GGAA motifs are indicated by black bars. Yellow highlighted area is 500 bp around the promoter region of Hes1. (E) Schematic representation of experiment shown in F-T′. Retinal explants were co-electroporated with either pCAG-GFP or pCAG-Ikzf4-IRES-GFP along with vectors expressing dsRed under the control of the wild-type Hes promoter (pHes1-dsRed) or the Hes1 promoter with a mutation at the first GGAA site (mut1), at the second GGAA site (mut2), at the third GGAA site (mut3), or at both second and third GGAA mutations (mut2+mut3). (F-T′) Photomicrographs of retinal flatmounts showing the increase in dsRed expression when Ikzf4-IRES-GFP is co-electroporated with pHes1-dsRed (F′,G′,H′), pHes1-mut1-dsRed (I′,J′,K′), pHes1-mut2-dsRed (L′,M′,N′) or pHes1-mut3-dsRed (O′,P′,Q′), but not with pHes1-mut2+3-dsRed (R′,S′,T′) compared with the control GFP. (U-W‴) Examples of P0 retinal explants electroporated with non-mutated pHes1-dsRed and either GFP (U,V,W,U″,V″,W″) or Ikzf4 (U′,V′,W′,U‴,V‴,W‴), followed by culturing for 3 days with DMSO (U-W′) or DAPT (U″-W‴), and explants fixed after 6 days *in vitro*. *n*=3 animals for all conditions except GFP+DAPT group (*n*=4). (X) Quantification of GFP$^+$ cells expressing DsRed at P0+6DIV after electroporation. ***P*<0.01, ****P*<0.001, *****P*<0.0001 (two-tailed unpaired *t*-test). RPL, retinal progenitor layer; DIV, days *in vitro*. Scale bars: 10 µm in A-B″,U-W‴; 250 µm in F-T′.

differentiation via two 'GGAA' Ikzf-binding sites in the promoter in a Notch signaling-dependent manner. Taken together, this study identifies redundancy between Ikaros family proteins and dynamic regulation of target gene selection as key mechanisms underlying temporal patterning in retinal progenitors (Fig. 7).

Ikzf1 and Ikzf4 in the control of cone development

Single knockout retinas of Ikzf1 or Ikzf4 have normal number of cones (Fig. 3C) (Elliott et al., 2008), but here we report that double knockouts of Ikzf1 and Ikzf4 have reduced cone numbers, suggesting redundant function for Ikzf1 and Ikzf4 in cone production. Alternatively, loss of Ikzf1 and Ikzf4 may only delay cone production, but the perinatal lethality of Ikzf1/Ikzf4 double knockouts prevented us from addressing this question. Future conditional inactivation should help circumvent this problem. Although we find that Ikzf1 and Ikzf4 bind different CREs, we also find co-binding at the same genes, suggesting that inactivation of one factor could be compensated by the other. It will be interesting to assess whether Ikzf1 switches binding profile upon loss of Ikzf4, and vice versa.

Our data indicate that Ikzf4 binds to and induces expression of *Pou2f2*, which suppresses the rod fate at early developmental stages, thereby favoring the cone fate. We observe an increase in Rxrg$^+$ cells and decrease of Nrl/Nr2e3$^+$ cells when Ikzf4 is overexpressed in late RPCs, suggesting that Ikzf4 is sufficient to reopen a window of competence for cone genesis that is normally lost at this stage. However, overexpression of Ikzf4 in late RPCs does not lead to the production of mature cones, unlike Pou2f1 (Javed et al., 2020), which suggests that it likely suppresses rod differentiation rather than promoting cone differentiation. We postulate that Ikzf4 might partially promote cone genesis, but additional factors required to promote full cone maturation are likely missing at late stages of retinogenesis. Ikzf4 also promotes early cell cycle exit, which is uncharacteristic of temporal identity factors such as Ikzf1, Pou2f1 and Casz1, but not Foxn4 (Elliott et al., 2008; Javed et al., 2020; Li et al., 2004; Mattar et al., 2015). Altogether, our results suggest that Ikzf4 is part of a gene regulatory network that confers RPCs with the competence to generate cones, possibly by repressing the rod fate at early stages.

Ikzf4 in the regulation of Müller glia production

Our data indicate that Ikzf4 switches transcriptional targets at late stages of retinogenesis to control Müller glia production. One possible mechanism to explain this switch is that Ikzf4 is co-expressed with Ikzf1 during early stages of retinal development, but not at late stages. The absence of Ikzf1 at late stages of development may redirect Ikzf4 from photoreceptor genes to glial genes, although such activity would have to be indirect because Ikzf1 and Ikzf4 have divergent genome occupancy. The current model of gliogenesis in the retina proposes that Nfia, Nfib

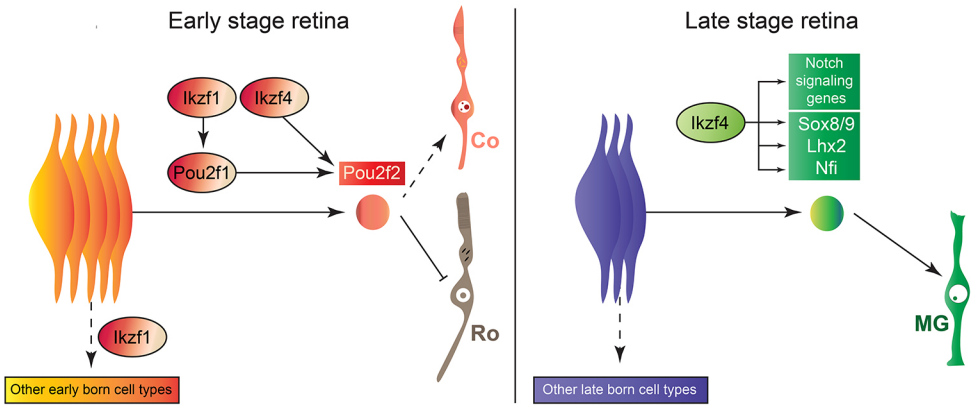

Fig. 7. Model of temporal patterning during mouse retinogenesis. In early RPCs, Ikzf4 functions redundantly with Ikzf1 to confer competence for cone (Co) production, either through suppression of the rod (Ro) fate by activating Pou2f2 or through upregulation of cone-specification genes, while Ikzf1 regulates competence to generate other early-born cell types. Alternatively, Ikzf1 and Ikzf4 might regulate the appropriate timing of cone differentiation during embryonic stages. Dashed line indicates the consequence of rod suppression, which leads to cone-like fate. In late RPCs, Ikzf4 contributes to Müller glia development by binding and upregulating expression of Müller specification genes, such as Notch signaling factors, *Sox8*, *Sox9*, *Lhx2* and the Nfi family, to ensure the Müller glia (MG) fate commitment. Ikzf4 may function in only a subset of RPCs. Additionally, Ikzf4 is expressed in some postmitotic cells and may have additional roles in these cells, which are not represented in this model.

Development (2023) 150, dev200436. doi:10.1242/dev.200436

and Nfix confer late-stage temporal identity to RPCs to generate Müller glia and bipolar cells (Clark et al., 2019; Lyu et al., 2021 preprint). In addition to Nfia, Nfib and Nfix, Lhx2 interacts with Rnf12 in late RPCs to promote gliogenesis by activating the expression of *Sox8* and/or *Sox9* and Notch target genes in postmitotic precursors destined to become Müller glia (de Melo et al., 2016, 2018; Jadhav et al., 2006; Muto et al., 2009; Nelson et al., 2011; Poché et al., 2008; Zhu et al., 2013; Zibetti et al., 2019). Lhx2 also dynamically alters its DNA-binding profile at early and late stages of retinal development to switch from promoting neurogenesis to promoting gliogenesis (Zibetti et al., 2019), as we observe here with Ikzf4. So how does Ikzf4 fit in the above proposed model of gliogenesis? As Lhx2, Nfia, Nfib and Nfix cKOs show no significant change in *Ikzf4* transcript levels (Clark et al., 2019; de Melo et al., 2016), and our data show that Ikzf4 binds to and induces expression of Lhx2 and Nfi, we propose that Ikzf4 may be upstream of these factors in the gliogenic gene regulatory network. Given the weak expression levels of *Ikzf4* and the low sensitivity of the RNA-seq analysis, however, it is possible that previous studies failed to detect changes in *Ikzf4* expression in the Lhx2 and Nfi cKOs. In any case, our data suggest a model wherein Ikzf4 favors the emergence of $Sox8^{+}$ and/or $Sox9^{+}$ precursors with sustained Notch signaling, as observed with the increase in $Hes1^{+}$ cells after overexpression of Ikzf4 in RPCs, which then go on to become Müller glia.

We report that Ikzf4 binds to regions close to many Notch signaling gene bodies, including multiple sites at the promoter of Hes1. Although we found an increase in *Hes1* mRNA levels after Ikzf4 overexpression, the reduction of *Hes1* expression observed in $Ikzf4^{-/-}$ retinas was not statistically significant compared with $Ikzf4^{+/-}$ (Fig. 5E), suggesting that Ikzf4 is sufficient but not completely necessary for *Hes1* expression. One possibility is that other Ikaros family members, such as Ikzf2 and Ikzf5 (Elliott et al., 2008), which are both expressed in the late developing mouse retina, are compensating to regulate *Hes1* expression. Another possibility is that Ikzf4 not only regulates *Hes1* but also several other Notch signaling factors to promote Müller glia. Consistently, we observe binding of Ikzf4 to other Notch signaling genes at P0, such as *Notch1* and *Rbpj* (Fig. 5A). Both *Hes5* and *Rbpj* mRNA level are significantly reduced in Ikzf4 KO retinas (Fig. 5E), suggesting a role for Ikzf4 in the regulation of several Notch signaling factors, which together may promote Müller glia development. As Hes1 promoter activation by Ikzf4 is impaired by blocking Notch signaling (Fig. 6X), the activation of the Notch pathway appears necessary for Ikzf4 to promote expression of *Hes1* and ultimately Müller glia development.

A broader role of Ikzf4 in cell fate specification

Previous studies have elucidated the role of Ikzf4 in the immune system. Most notably, Ikzf4 function in T-cell differentiation varies considerably depending on $CD4^{+}$ T-cell subtype, highlighting the dynamic role of Ikzf4 function based on the cellular context (Liu et al., 2014; Pan et al., 2009; Powell et al., 2019; Read et al., 2017; Rieder et al., 2015; Sekiya et al., 2015; Sharma et al., 2013), similar to what we report here. Interestingly, widespread expression of Ikzf4 has been reported in different organs, including the CNS (Perdomo et al., 2000). One study has detailed the role of Ikzf4 in regulating expression of PSD-95 in adult cochlear afferent neurons (Bao et al., 2004), but the function of Ikzf4 in the developing CNS remains largely elusive. The findings reported here suggest that Ikzf4 may have widespread regulatory functions in the CNS to control cell fate specification. Future studies on conditional knockouts of Ikzf4 alone or in combination with other Ikzf genes will be interesting to address this issue.

MATERIALS AND METHODS

Animals

All experiments were carried out in accordance with the Canadian Council on Animal guidelines and approved by the IRCM animal care committee. Ikzf1 (Wang et al., 1996) and Ikzf4 (International Mouse Phenotyping Consortium and RIKEN Bioresource RRID: IMSR_RBRC06808) knockout mice were raised in the C57BL/6J background (*Mus musculus*). All other mouse experiments were performed on wild-type CD1 mice (*Mus musculus*, Charles River Laboratories). Animals of either sex were used in this study.

Retroviral constructs preparation and retinal explant culture

Retroviruses were designed, produced and concentrated as previously described (Cayouette et al., 2003). Retinal explants were cultured as previously outlined (Cayouette et al., 2001). Retroviral infections of retinal explants and analyses of the retroviral clones were carried out as previously stated (Javed et al., 2020). Retinal explants were fixed either 2, 3, 6, 12 or 14 days after electroporation, as required for the experiment, and processed for immunostaining. For the Notch signaling inhibition experiment, DMSO or DAPT was added to the medium as previously described at concentration of 10 µM for the first 3 days of culture, and explants fixed after 6 days *in vitro* (Nelson et al., 2011).

Plasmid and mutation cloning

Ikzf1 and Ikzf4 cDNAs were cloned into a pCIG2-IRES-GFP and pCLE-venus vector using restriction sites previously outlined (Gaiano et al., 2000; Hand et al., 2005). pHes1-dsRed vector was mutated with Infusion HD Cloning Plus kit from Takara using primers listed in Table S1 (Matsuda and Cepko, 2007).

In vivo electroporation

P0 or P1 eyes were injected with DNA plasmid at 3 µg/µl concentration containing 0.5% Fast Green and electroporated as previously described (de Melo and Blackshaw, 2011).

RNA isolation and quantitative PCR

RNA extraction and qPCR quantitation were performed as previously described (Javed et al., 2020). Primers used are listed in Table S9 (Batsché et al., 2005; Ouimette et al., 2010).

RNA-seq preparation

P0 CD1 retinas were dissociated using Accutase and transfected using the Amaxa Neural Stem Cell Kit according to the manufacturer's protocol. Cells were seeded into six-well plates coated with PLL/Laminin, and cultured as previously described (Gomes et al., 2011). After 9 h, cells were harvested and dissociated with Accutase followed by FAC-sorting for GFP. Control GFP condition contained 4×10^{5} cells per biological replicate (n=4) and Ikzf1 condition contained 3×10^{5} cells per biological replicate (n=4). Cells were sorted directly into lysis buffer and purified using the RNeasy micro kit from Qiagen. Sample quantity (RNA integrity number=RIN) and quality were assessed using the Agilent RNA 6000 Pico Kit (Agilent 5067-1513) on the Bioanalyzer 2100. rRNA was depleted using Ribo-Zero Magnetic Gold Kit for rRNA depletion (Human/Mouse/Rat) (Epicentre for Illumina, MRZG12324) according to the manufacturer's guidelines. Library preparations were made out using SMARTer Stranded RNA-Seq Kit (Clontech, 634836 or 634837) according to the manufacturer's guidelines. Libraries were diluted and pooled equimolarly, and then sequenced in pair end 50 cycles (PE50) on a v4 flowcell (Illumina HiSeq PE Cluster Kit v4 cBot, PE-401-4001) of the Illumina HiSeq 2500 System.

Tissue collection and immunofluorescence

The age of mouse embryos was calculated from pregnant females with the day of vaginal plug considered as day 0 (E0) and collected at E11, E14, E15, E16, E17, P0, P2 and P7 for spatiotemporal analyses. For endogenous Ikzf1

Development (2023) 150, dev200436. doi:10.1242/dev.200436

and Ikzf4 immunostaining, the retinas were dissected and fixed for 2 min in 4%PFA/PBS followed by immersion in 20% sucrose/PBS for 1 h. Retinas were then embedded in OCT, frozen in liquid nitrogen, sectioned at 25 µm using a cryostat and immunostained on the same day. For all other antibodies and Ikzf4 immunostaining against overexpressed Ikzf4 protein, the decapitated heads from embryos or eyes from postnatal pups were fixed for 15 min in 4%PFA/PBS and immersed in 20% sucrose/PBS for 2 h.

Immunofluorescence was performed as previously described (Javed et al., 2020). A list of primary antibodies can be found in Table S10, including DHSB antibodies (Venkataraman et al., 2018).

EdU labeling assay

EdU (30 µM) was added to the culture medium for 2 h before collection and fixation. Click-iT EdU Alexa Fluor 647 was used to label cells that incorporated EdU.

Statistical and quantitative analyses

Statistical tests were performed for each experiment in this study, as indicated in the figure legends. All quantifications in the bar graphs of this study are represented as mean±standard error of the mean (s.e.m.), whereas *n* number and individual values on the graphs represent biological replicates. Statistics for the retroviral clonal analyses were performed as previously outlined (Pounds and Dyer, 2008). Retinal explants containing disorganized layers and poor immunostainings were discarded and analysis was limited to the well-organized regions of the retinal explants. All experiments were repeated at least three times.

Ikzf4 knockouts were analyzed as follows. Two sections of P10 central retinas oriented temporo-nasally were examined with quantifications of 200 µm (Pax6), 400 µm (Otx2, Sox2 and Lhx2 staining in the INL, Rxrg in the ONL) and 800 µm (Brn3a and Lim-1) lengths of the imaged section. The investigator was blinded to the genotype of animals. An ImageJ analysis macro was written to count cells automatically in a section. Analyze particles in ImageJ was used after defining a region of interest and setting threshold for each antibody to auto-count cell numbers of $Pax6^{+}$, $Otx2^{+}$, $Sox2^{+ve}$, $Lhx2^{+}$ and $Brn3a^{+}$ cells, whereas $Rxrg^{+}$ and $Lim\text{-}1^{+}$ cells were manually counted. Ikzf1/4 double knockouts were analyzed as follows. Three sections of E15 central retinas in embryonic heads oriented dorso-ventrally were analyzed with quantification of 200 µm for $Rxrg^{+}$ cells and 400 µm for $Brn3a^{+}$ cells. $Rxrg^{+}$ cells were manually counted due to background signal, whereas $Brn3a^{+}$ cells were counted using the ImageJ analysis macro as described above. All cell quantifications were performed by blinding the investigators to the genotype of the animals.

CUT&RUN assays

CUT&RUN was performed as previously described (Skene et al., 2018), with a few added modifications. For Ikzf1 CUT&RUN, CAG-Ikzf1 electroporated P0 retinal explants were cultured and 50,000 GFP^{+} cells were sorted directly into the buffer with Concanavalin A beads. For Ikzf4 CUT&RUN, E14 and P0 retinas were dissected, and 1,500,000 cells were used for each stage. The entire procedure was carried out in 200 µl PCR tubes. Digitonin at 0.01% concentration was used and pAG-MNase digestion was performed for 30 min on ice.

Libraries were prepared with the KAPA DNA HyperPrep Kit (Roche 07962363001 - KK8504). This protocol includes an End-Repair/A-tailing step and an adapter ligation step followed by a PCR amplification (enrichment) of ligated fragments. The adapters used for ligation were IDT for Illumina TruSeq UD Indexes (Illumina - 20022371). The final enriched product (library, after PCR) was purified using KAPA purification beads (Roche 07983298001 - KK8002) and a dual-SPRI size selection was performed (with KAPA beads) to select fragments between 180-500 bp. Libraries were then quantified using a Nanodrop microvolume spectrophotometer (ng/µl) and quality was assessed using the Agilent High Sensitivity DNA Kit (Agilent - 5067-4626) on a Bioanalyzer 2100. The libraries were then quantified by q-PCR to obtain their nanomolar (nM) concentration. Libraries were diluted, pooled equimolar and sequenced in pair end 50 cycles (PE50) on a S1 flowcell (Illumina - 20012863) of the Illumina NovaSeq 6000 System.

Bioinformatics analyses

scRNA-seq analyses of previously published datasets was performed as follows. Fastq raw reads were aligned and counted to generate matrices for each individual stage from Mouse retina atlas (GEO: GSE118614) (Clark et al., 2019) and Human fetal retina atlas (GEO: GSE116106, GSE122970 and GSE138002) (Lu et al., 2020) using Cellranger 4.0 (10x Genomics). Velocyto (La Manno et al., 2018) with run10x function was used on cellranger output folders to generate loom files for each individual stages. Seurat (Butler et al., 2018) was used to analyze the mouse and human retina loom files and subset RPC clusters for Ikzf4/IKZF4 expression analyses using markers previously described (Clark et al., 2019; Lu et al., 2020). Scanpy (Wolf et al., 2018) was used to analyze the same loom files and generate Ikzf4/IKZF4 expression UMAPs along with cell type markers (Fig. S2).

RNA-seq fastq raw reads were analyzed using the salmon quantification package (Patro et al., 2017). Differential gene expression analyses between CAG-GFP and CAG-Ikzf1 was performed using DESeq2 on Salmon quant output files (Love et al., 2014). R intersect() function was used to compare differentially expressed gene lists with Ikzf1 CUT&RUN peaks.

CUT&RUN analyses were performed by aligning the raw fastq reads with the mouse mm9 genome using default parameters of bowtie2 on Galaxy platform (Afgan et al., 2016; Langmead and Salzberg, 2012). Bam files generated for Ikzf4 and IgG CUT&RUN at each stage were used to call peaks using 0.5 FDR parameter on MACS2 (Feng et al., 2012). Bedtools was used to find overlapping peaks between the two stages (Quinlan and Hall, 2010). Bigwig files were generated using deeptools2 (Ramírez et al., 2016). Integrative Genomics Viewer (IGV) was used to visualize bigwig files.

TOBIAS footprinting analysis was performed by first intersecting ATAC-seq peaks at E14 and P0 from previously published datasets (Aldiri et al., 2017), with Ikzf4 E14 and P0 regions using bedtools (Bentsen et al., 2020; Quinlan and Hall, 2010). TOBIAS ATACorrect and ScoreBigwig was performed on ATAC-seq E14 and P0 bam files separately to generate corrected ATAC-seq bigwig files. The two E14 and P0 regions were merged using bedtools, and BINDetect was used to estimate differentially bound motifs based on scores, sequence and motifs. The JASPAR non-redundant vertebrate motifs package was used for motif annotation on the mm9 genome (Fornes et al., 2020).

Volcano plots were generated using the EnhancedVolcanoplot github package (https://github.com/kevinblighe/EnhancedVolcano), whereas Upset plots were generated using Upsetplot shiny web tool (Conway et al., 2017). Information on each software version is listed in Table S10.

Acknowledgements

We thank Christine Jolicoeur for technical assistance; Jessica Barthe and Androne Constantin from the IRCM animal core facility; Odile Neyret-Djossou from the IRCM molecular biology platform; and Éric Massicotte and Julie Lord from the IRCM flow cytometry platform. We thank Seth Blackshaw for critical comments on the manuscript. We thank Aurelie Huang-Sung and Nicole Francis for providing the pAG-Mnase for the CUT&RUN experiments. We thank Benoit Boulan for writing the ImageJ macro. We also thank all members of the Cayouette lab and Shahrzad Bahrampour for their comments and support.

Competing interests

The authors declare no competing or financial interests.

Author contributions

Conceptualization: A.J., P.L.S.-F., P.M., M.C.; Methodology: A.J.; Investigation: A.J., P.L.S.-F., P.M., A.C., F.K.; Data curation: A.J., P.L.S.-F., P.M., A.C., M.C.; Writing - original draft: A.J.; Writing - review & editing: P.L.S.-F., P.M., M.C.; Visualization: A.J.; Supervision: M.C.; Project administration: M.C.; Funding acquisition: M.C.

Funding

This project was funded by grants from the Canadian Institutes of Health Research (FDN-159936) and Fighting Blindness Canada to M.C. A.J. was supported by a PhD scholarship from the Fonds de recherche du Québec – Santé. M.C. is an Emeritus Scholar from Fonds de recherche du Québec – Santé and holds the Gaëtane and Rolland Pillenière Chair in Retinal Biology from the Montreal Clinical Research Institute Foundation.

Data availability

E14 IgG CUT&RUN raw reads are from a previously published GEO dataset (accession number GSE156756; Brodie-Kommit et al., 2021). Processed RNA-seq, MACS2 peaks and bigwig files have been deposited in GEO under accession number GSE189590.

Peer review history

The peer review history is available online at https://journals.biologists.com/dev/lookup/doi/10.1242/dev.200436.reviewer-comments.pdf

References

Afgan, E., Baker, D., van den Beek, M., Blankenberg, D., Bouvier, D., Čech, M., Chilton, J., Clements, D., Coraor, N., Eberhard, C. et al. (2016). The Galaxy platform for accessible, reproducible and collaborative biomedical analyses: 2016 update. *Nucleic Acids Res.* **44**, W3-W10. doi:10.1093/nar/gkw343

Aldiri, I., Xu, B., Wang, L., Chen, X., Hiler, D., Griffiths, L., Valentine, M., Shirinifard, A., Thiagarajan, S., Sablauer, A. et al. (2017). The dynamic epigenetic landscape of the retina during development, reprogramming, and tumorigenesis. *Neuron* **94**, 550-568.e510. doi:10.1016/j.neuron.2017.04.022

Bao, J., Lin, H., Ouyang, Y., Lei, D., Osman, A., Kim, T.-W., Mei, L., Dai, P., Ohlemiller, K. K. and Ambron, R. T. (2004). Activity-dependent transcription regulation of PSD-95 by neuregulin-1 and Eos. *Nat. Neurosci.* **7**, 1250-1258. doi:10.1038/nn1342

Batsché, E., Moschopoulos, P., Desroches, J., Bilodeau, S. and Drouin, J. (2005). Retinoblastoma and the related pocket protein p107 act as coactivators of NeuroD1 to enhance gene transcription. *J. Biol. Chem.* **280**, 16088-16095. doi:10.1074/jbc.M413427200

Bentsen, M., Goymann, P., Schultheis, H., Klee, K., Petrova, A., Wiegandt, R., Fust, A., Preussner, J., Kuenne, C., Braun, T. et al. (2020). ATAC-seq footprinting unravels kinetics of transcription factor binding during zygotic genome activation. *Nat. Commun.* **11**, 4267. doi:10.1038/s41467-020-18035-1

Blackshaw, S., Harpavat, S., Trimarchi, J., Cai, L., Huang, H., Kuo, W. P., Weber, G., Lee, K., Fraioli, R. E., Cho, S. H. et al. (2004). Genomic analysis of mouse retinal development. *PLoS Biol.* **2**, E247. doi:10.1371/journal.pbio.0020247

Brodie-Kommit, J., Clark, B. S., Shi, Q., Shiau, F., Kim, D. W., Langel, J., Sheely, C., Ruzycki, P. A., Fries, M., Javed, A. et al. (2021). Atoh7-independent specification of retinal ganglion cell identity. *Sci. Adv.* **7**, abe4983. doi:10.1126/sciadv.abe4983

Brody, T. and Odenwald, W. F. (2000). Programmed transformations in neuroblast gene expression during Drosophila CNS lineage development. *Dev. Biol.* **226**, 34-44. doi:10.1006/dbio.2000.9829

Butler, A., Hoffman, P., Smibert, P., Papalexi, E. and Satija, R. (2018). Integrating single-cell transcriptomic data across different conditions, technologies, and species. *Nat. Biotechnol.* **36**, 411-420. doi:10.1038/nbt.4096

Cao, R., Wang, L., Wang, H., Xia, L., Erdjument-Bromage, H., Tempst, P., Jones, R. S. and Zhang, Y. (2002). Role of histone H3 lysine 27 methylation in Polycomb-group silencing. *Science* **298**, 1039-1043. doi:10.1126/science.1076997

Carter-Dawson, L. D. and LaVail, M. M. (1979a). Rods and cones in the mouse retina. I. Structural analysis using light and electron microscopy. *J. Comp. Neurol.* **188**, 245-262. doi:10.1002/cne.901880204

Carter-Dawson, L. D. and LaVail, M. M. (1979b). Rods and cones in the mouse retina. II. Autoradiographic analysis of cell generation using tritiated thymidine. *J. Comp. Neurol.* **188**, 263-272. doi:10.1002/cne.901880205

Cayouette, M., Whitmore, A. V., Jeffery, G. and Raff, M. (2001). Asymmetric segregation of Numb in retinal development and the influence of the pigmented epithelium. *J. Neurosci.* **21**, 5643-5651. doi:10.1523/JNEUROSCI.21-15-05643.2001

Cayouette, M., Barres, B. A. and Raff, M. (2003). Importance of intrinsic mechanisms in cell fate decisions in the developing rat retina. *Neuron* **40**, 897-904. doi:10.1016/S0896-6273(03)00756-6

Clark, B. S., Stein-O'Brien, G. L., Shiau, F., Cannon, G. H., Davis-Marcisak, E., Sherman, T., Santiago, C. P., Hoang, T. V., Rajaii, F., James-Esposito, R. E. et al. (2019). Single-cell RNA-seq analysis of retinal development identifies NFI factors as regulating mitotic exit and late-born cell specification. *Neuron* **102**, 1111-1126.e1115. doi:10.1016/j.neuron.2019.04.010

Cleary, M. D. and Doe, C. Q. (2006). Regulation of neuroblast competence: multiple temporal identity factors specify distinct neuronal fates within a single early competence window. *Genes Dev.* **20**, 429-434. doi:10.1101/gad.1382206

Conway, J. R., Lex, A. and Gehlenborg, N. (2017). UpSetR: an R package for the visualization of intersecting sets and their properties. *Bioinformatics* **33**, 2938-2940. doi:10.1093/bioinformatics/btx364

Creyghton, M. P., Cheng, A. W., Welstead, G. G., Kooistra, T., Carey, B. W., Steine, E. J., Hanna, J., Lodato, M. A., Frampton, G. M., Sharp, P. A. et al. (2010). Histone H3K27ac separates active from poised enhancers and predicts developmental state. *Proc. Natl. Acad. Sci. USA* **107**, 21931-21936. doi:10.1073/pnas.1016071107

Davis, N., Mor, E. and Ashery-Padan, R. (2011). Roles for Dicer1 in the patterning and differentiation of the optic cup neuroepithelium. *Development* **138**, 127-138. doi:10.1242/dev.053637

de Melo, J. and Blackshaw, S. (2011). In vivo electroporation of developing mouse retina. *J. Vis. Exp.* **24**, 2847. doi:10.3791/2847

de Melo, J., Peng, G.-H., Chen, S. and Blackshaw, S. (2011). The Spalt family transcription factor Sall3 regulates the development of cone photoreceptors and retinal horizontal interneurons. *Development* **138**, 2325-2336. doi:10.1242/dev.061846

de Melo, J., Zibetti, C., Clark, B. S., Hwang, W., Miranda-Angulo, A. L., Qian, J. and Blackshaw, S. (2016). Lhx2 is an essential factor for retinal gliogenesis and Notch signaling. *J. Neurosci.* **36**, 2391-2405. doi:10.1523/JNEUROSCI.3145-15.2016

de Melo, J., Clark, B. S., Venkataraman, A., Shiau, F., Zibetti, C. and Blackshaw, S. (2018). Ldb1- and Rnf12-dependent regulation of Lhx2 controls the relative balance between neurogenesis and gliogenesis in the retina. *Development* **145**, dev159970. doi:10.1242/dev.159970

Decembrini, S., Bressan, D., Vignali, R., Pitto, L., Mariotti, S., Rainaldi, G., Wang, X., Evangelista, M., Barsacchi, G. and Cremisi, F. (2009). MicroRNAs couple cell fate and developmental timing in retina. *Proc. Natl. Acad. Sci. USA* **106**, 21179-21184. doi:10.1073/pnas.0909167106

Dupacova, N., Antosova, B., Paces, J. and Kozmik, Z. (2021). Meis homeobox genes control progenitor competence in the retina. *Proc. Natl. Acad. Sci. USA* **118**, e2013136118. doi:10.1073/pnas.2013136118

Elliott, J., Jolicoeur, C., Ramamurthy, V. and Cayouette, M. (2008). Ikaros confers early temporal competence to mouse retinal progenitor cells. *Neuron* **60**, 26-39. doi:10.1016/j.neuron.2008.08.008

Emerson, M. M., Surzenko, N., Goetz, J. J., Trimarchi, J. and Cepko, C. L. (2013). Otx2 and Onecut1 promote the fates of cone photoreceptors and horizontal cells and repress rod photoreceptors. *Dev. Cell* **26**, 59-72. doi:10.1016/j.devcel.2013.06.005

Erclik, T., Li, X., Courgeon, M., Bertet, C., Chen, Z., Baumert, R., Ng, J., Koo, C., Arain, U., Behnia, R. et al. (2017). Integration of temporal and spatial patterning generates neural diversity. *Nature* **541**, 365-370. doi:10.1038/nature20794

Feng, J., Liu, T., Qin, B., Zhang, Y. and Liu, X. S. (2012). Identifying ChIP-seq enrichment using MACS. *Nat. Protoc.* **7**, 1728-1740. doi:10.1038/nprot.2012.101

Fornes, O., Castro-Mondragon, J. A., Khan, A., van der Lee, R., Zhang, X., Richmond, P. A., Modi, B. P., Correard, S., Gheorghe, M., Baranašić, D. et al. (2020). JASPAR 2020: update of the open-access database of transcription factor binding profiles. *Nucleic Acids Res.* **48**, D87-D92. doi:10.1093/nar/gkz1001

Furukawa, T., Mukherjee, S., Bao, Z.-Z., Morrow, E. M. and Cepko, C. L. (2000). rax, Hes1, and notch1 promote the formation of Muller glia by postnatal retinal progenitor cells. *Neuron* **26**, 383-394. doi:10.1016/S0896-6273(00)81171-X

Gaiano, N., Nye, J. S. and Fishell, G. (2000). Radial glial identity is promoted by Notch1 signaling in the murine forebrain. *Neuron* **26**, 395-404. doi:10.1016/S0896-6273(00)81172-1

Georgi, S. A. and Reh, T. A. (2010). Dicer is required for the transition from early to late progenitor state in the developing mouse retina. *J. Neurosci.* **30**, 4048-4061. doi:10.1523/JNEUROSCI.4982-09.2010

Gomes, F. L. A. F., Zhang, G., Carbonell, F., Correa, J. A., Harris, W. A., Simons, B. D. and Cayouette, M. (2011). Reconstruction of rat retinal progenitor cell lineages in vitro reveals a surprising degree of stochasticity in cell fate decisions. *Development* **138**, 227-235. doi:10.1242/dev.059683

Gordon, P. J., Yun, S., Clark, A. M., Monuki, E. S., Murtaugh, L. C. and Levine, E. M. (2013). Lhx2 balances progenitor maintenance with neurogenic output and promotes competence state progression in the developing retina. *J. Neurosci.* **33**, 12197-12207. doi:10.1523/JNEUROSCI.1494-13.2013

Grosskortenhaus, R., Pearson, B. J., Marusich, A. and Doe, C. Q. (2005). Regulation of temporal identity transitions in Drosophila neuroblasts. *Dev. Cell* **8**, 193-202. doi:10.1016/j.devcel.2004.11.019

Grosskortenhaus, R., Robinson, K. J. and Doe, C. Q. (2006). Pdm and Castor specify late-born motor neuron identity in the NB7-1 lineage. *Genes Dev.* **20**, 2618-2627. doi:10.1101/gad.1445306

Hand, R., Bortone, D., Mattar, P., Nguyen, L., Heng, J. I.-T., Guerrier, S., Boutt, E., Peters, E., Barnes, A. P., Parras, C. et al. (2005). Phosphorylation of Neurogenin2 specifies the migration properties and the dendritic morphology of pyramidal neurons in the neocortex. *Neuron* **48**, 45-62. doi:10.1016/j.neuron.2005.08.032

He, J., Zhang, G., Almeida, A. D., Cayouette, M., Simons, B. D. and Harris, W. A. (2012). How variable clones build an invariant retina. *Neuron* **75**, 786-798. doi:10.1016/j.neuron.2012.06.033

Heinz, S., Benner, C., Spann, N., Bertolino, E., Lin, Y. C., Laslo, P., Cheng, J. X., Murre, C., Singh, H. and Glass, C. K. (2010). Simple combinations of lineage-determining transcription factors prime cis-regulatory elements required for macrophage and B cell identities. *Mol. Cell* **38**, 576-589. doi:10.1016/j.molcel.2010.05.004

Hojo, M., Ohtsuka, T., Hashimoto, N., Gradwohl, G., Guillemot, F. and Kageyama, R. (2000). Glial cell fate specification modulated by the bHLH gene Hes5 in mouse retina. *Development* **127**, 2515-2522. doi:10.1242/dev.127.12.2515

Iida, A., Shinoe, T., Baba, Y., Mano, H. and Watanabe, S. (2011). Dicer plays essential roles for retinal development by regulation of survival and differentiation. *Invest. Ophthalmol. Vis. Sci.* **52**, 3008-3017. doi:10.1167/iovs.10-6428

Imayoshi, I., Isomura, A., Harima, Y., Kawaguchi, K., Kori, H., Miyachi, H., Fujiwara, T., Ishidate, F. and Kageyama, R. (2013). Oscillatory control of factors determining multipotency and fate in mouse neural progenitors. *Science* **342**, 1203-1208. doi:10.1126/science.1242366

Isshiki, T., Pearson, B., Holbrook, S. and Doe, C. Q. (2001). Drosophila neuroblasts sequentially express transcription factors which specify the temporal identity of their neuronal progeny. *Cell* **106**, 511-521. doi:10.1016/S0092-8674(01)00465-2

Jadhav, A. P., Cho, S.-H. and Cepko, C. L. (2006). Notch activity permits retinal cells to progress through multiple progenitor states and acquire a stem cell property. *Proc. Natl. Acad. Sci. USA* **103**, 18998-19003. doi:10.1073/pnas.0608155103

Javed, A., Mattar, P., Lu, S., Kruczek, K., Kloc, M., Gonzalez-Cordero, A., Bremner, R., Ali, R. R. and Cayouette, M. (2020). Pou2f1 and Pou2f2 cooperate to control the timing of cone photoreceptor production in the developing mouse retina. *Development* **147**, dev188730. doi:10.1242/dev.188730

Jean-Charles, N., Buenaventura, D. F. and Emerson, M. M. (2018). Identification and characterization of early photoreceptor cis-regulatory elements and their relation to Onecut1. *Neural Dev.* **13**, 26. doi:10.1186/s13064-018-0121-x

Kambadur, R., Koizumi, K., Stivers, C., Nagle, J., Poole, S. J. and Odenwald, W. F. (1998). Regulation of POU genes by castor and hunchback establishes layered compartments in the Drosophila CNS. *Genes Dev.* **12**, 246-260. doi:10.1101/gad.12.2.246

La Manno, G., Soldatov, R., Zeisel, A., Braun, E., Hochgerner, H., Petukhov, V., Lidschreiber, K., Kastriti, M. E., Lönnerberg, P., Furlan, A. et al. (2018). RNA velocity of single cells. *Nature* **560**, 494-498. doi:10.1038/s41586-018-0414-6

La Torre, A., Georgi, S. and Reh, T. A. (2013). Conserved microRNA pathway regulates developmental timing of retinal neurogenesis. *Proc. Natl. Acad. Sci. USA* **110**, E2362-E2370. doi:10.1073/pnas.1301837110

Langmead, B. and Salzberg, S. L. (2012). Fast gapped-read alignment with Bowtie 2. *Nat. Methods* **9**, 357-359. doi:10.1038/nmeth.1923

Li, S., Mo, Z., Yang, X., Price, S. M., Shen, M. M. and Xiang, M. (2004). Foxn4 controls the genesis of amacrine and horizontal cells by retinal progenitors. *Neuron* **43**, 795-807. doi:10.1016/j.neuron.2004.08.041

Li, X., Erclik, T., Bertet, C., Chen, Z., Voutev, R., Venkatesh, S., Morante, J., Celik, A. and Desplan, C. (2013). Temporal patterning of Drosophila medulla neuroblasts controls neural fates. *Nature* **498**, 456-462. doi:10.1038/nature12319

Lin, Y.-P., Ouchi, Y., Satoh, S. and Watanabe, S. (2009). Sox2 plays a role in the induction of amacrine and Müller glial cells in mouse retinal progenitor cells. *Invest. Ophthalmol. Vis. Sci.* **50**, 68-74. doi:10.1167/iovs.07-1619

Liu, S.-Q., Jiang, S., Li, C., Zhang, B. and Li, Q.-J. (2014). miR-17-92 cluster targets phosphatase and tensin homology and Ikaros Family Zinc Finger 4 to promote TH17-mediated inflammation. *J. Biol. Chem.* **289**, 12446-12456. doi:10.1074/jbc.M114.550723

Liu, S., Liu, X., Li, S., Huang, X., Qian, H., Jin, K. and Xiang, M. (2020). Foxn4 is a temporal identity factor conferring mid/late-early retinal competence and involved in retinal synaptogenesis. *Proc. Natl. Acad. Sci. USA* **117**, 5016-5027. doi:10.1073/pnas.1918628117

Livne-bar, I., Pacal, M., Cheung, M. C., Hankin, M., Trogadis, J., Chen, D., Dorval, K. M. and Bremner, R. (2006). Chx10 is required to block photoreceptor differentiation but is dispensable for progenitor proliferation in the postnatal retina. *Proc. Natl. Acad. Sci. USA* **103**, 4988-4993. 10.1073/pnas.0600083103

Love, M. I., Huber, W. and Anders, S. (2014). Moderated estimation of fold change and dispersion for RNA-seq data with DESeq2. *Genome Biol.* **15**, 550. doi:10.1186/s13059-014-0550-8

Lu, Y., Shiau, F., Yi, W., Lu, S., Wu, Q., Pearson, J. D., Kallman, A., Zhong, S., Hoang, T., Zuo, Z. et al. (2020). Single-cell analysis of human retina identifies evolutionarily conserved and species-specific mechanisms controlling development. *Dev. Cell* **53**, 473-491.e479. doi:10.1016/j.devcel.2020.04.009

Lyu, P., Hoang, T., Santiago, C. P., Thomas, E. D., Timms, A. E., Appel, H., Gimmen, M., Le, N., Jiang, L., Kim, D. W. et al. (2021). Gene regulatory networks controlling temporal patterning, neurogenesis, and cell fate specification in the mammalian retina. *Cell Reports* **37**, 109994. doi:10.1016/j.celrep.2021.109994

Matsuda, T. and Cepko, C. L. (2007). Controlled expression of transgenes introduced by in vivo electroporation. *Proc. Natl. Acad. Sci. USA* **104**, 1027-1032. doi:10.1073/pnas.0610155104

Mattar, P. and Cayouette, M. (2015). Mechanisms of temporal identity regulation in mouse retinal progenitor cells. *Neurogenesis (Austin)* **2**, e1125409. doi:10.1080/23262133.2015.1125409

Mattar, P., Ericson, J., Blackshaw, S. and Cayouette, M. (2015). A conserved regulatory logic controls temporal identity in mouse neural progenitors. *Neuron* **85**, 497-504. doi:10.1016/j.neuron.2014.12.052

McLean, C. Y., Bristor, D., Hiller, M., Clarke, S. L., Schaar, B. T., Lowe, C. B., Wenger, A. M. and Bejerano, G. (2010). GREAT improves functional interpretation of cis-regulatory regions. *Nat. Biotechnol.* **28**, 495-501. doi:10.1038/nbt.1630

Molnár, A. and Georgopoulos, K. (1994). The Ikaros gene encodes a family of functionally diverse zinc finger DNA-binding proteins. *Mol. Cell. Biol.* **14**, 8292-8303. doi:10.1128/mcb.14.12.8292-8303.1994

Mori, M., Ghyselinck, N. B., Chambon, P. and Mark, M. (2001). Systematic immunolocalization of retinoid receptors in developing and adult mouse eyes. *Invest. Ophthalmol. Vis. Sci.* **42**, 1312-1318.

Muto, A., Iida, A., Satoh, S. and Watanabe, S. (2009). The group E Sox genes Sox8 and Sox9 are regulated by Notch signaling and are required for Muller glial cell development in mouse retina. *Exp. Eye Res.* **89**, 549-558. doi:10.1016/j.exer.2009.05.006

Nelson, B. R., Ueki, Y., Reardon, S., Karl, M. O., Georgi, S., Hartman, B. H., Lamba, D. A. and Reh, T. A. (2011). Genome-wide analysis of Müller glial differentiation reveals a requirement for Notch signaling in postmitotic cells to maintain the glial fate. *PLoS ONE* **6**, e22817-e22817. doi:10.1371/journal.pone.0022817

Ng, L., Hurley, J. B., Dierks, B., Srinivas, M., Salto, C., Vennström, B., Reh, T. A. and Forrest, D. (2001). A thyroid hormone receptor that is required for the development of green cone photoreceptors. *Nat. Genet.* **27**, 94-98. doi:10.1038/83829

Novotny, T., Eiselt, R. and Urban, J. (2002). Hunchback is required for the specification of the early sublineage of neuroblast 7-3 in the Drosophila central nervous system. *Development* **129**, 1027-1036. doi:10.1242/dev.129.4.1027

Orford, K., Kharchenko, P., Lai, W., Dao, M. C., Worhunsky, D. J., Ferro, A., Janzen, V., Park, P. J. and Scadden, D. T. (2008). Differential H3K4 methylation identifies developmentally poised hematopoietic genes. *Dev. Cell* **14**, 798-809. doi:10.1016/j.devcel.2008.04.002

Ouimette, J.-F., Jolin, M. L., L'Honore, A., Gifuni, A. and Drouin, J. (2010). Divergent transcriptional activities determine limb identity. *Nat. Commun.* **1**, 35. doi:10.1038/ncomms1036

Pan, F., Yu, H., Dang, E. V., Barbi, J., Pan, X., Grosso, J. F., Jinasena, D., Sharma, S. M., McCadden, E. M., Getnet, D. et al. (2009). Eos mediates Foxp3-dependent gene silencing in CD4+ regulatory T cells. *Science* **325**, 1142-1146. doi:10.1126/science.1176077

Patro, R., Duggal, G., Love, M. I., Irizarry, R. A. and Kingsford, C. (2017). Salmon provides fast and bias-aware quantification of transcript expression. *Nat. Methods* **14**, 417-419. doi:10.1038/nmeth.4197

Pearson, B. J. and Doe, C. Q. (2003). Regulation of neuroblast competence in Drosophila. *Nature* **425**, 624-628. doi:10.1038/nature01910

Perdomo, J., Holmes, M., Chong, B. and Crossley, M. (2000). Eos and pegasus, two members of the Ikaros family of proteins with distinct DNA binding activities. *J. Biol. Chem.* **275**, 38347-38354. doi:10.1074/jbc.M005457200

Poché, R. A., Furuta, Y., Chaboissier, M.-C., Schedl, A. and Behringer, R. R. (2008). Sox9 is expressed in mouse multipotent retinal progenitor cells and functions in Muller glial cell development. *J. Comp. Neurol.* **510**, 237-250. doi:10.1002/cne.21746

Pomaznoy, M., Ha, B. and Peters, B. (2018). GOnet: a tool for interactive Gene Ontology analysis. *BMC Bioinformatics* **19**, 470. doi:10.1186/s12859-018-2533-3

Pounds, S. and Dyer, M. A. (2008). Statistical analysis of data from retroviral clonal experiments in the developing retina. *Brain Res.* **1192**, 178-185. doi:10.1016/j.brainres.2007.08.074

Powell, M. D., Read, K. A., Sreekumar, B. K. and Oestreich, K. J. (2019). Ikaros zinc finger transcription factors: regulators of cytokine signaling pathways and CD4(+) T helper cell differentiation. *Front. Immunol.* **10**, 1299. doi:10.3389/fimmu.2019.01299

Quinlan, A. R. and Hall, I. M. (2010). BEDTools: a flexible suite of utilities for comparing genomic features. *Bioinformatics* **26**, 841-842. doi:10.1093/bioinformatics/btq033

Ramírez, F., Ryan, D. P., Grüning, B., Bhardwaj, V., Kilpert, F., Richter, A. S., Heyne, S., Dündar, F. and Manke, T. (2016). deepTools2: a next generation web server for deep-sequencing data analysis. *Nucleic Acids Res.* **44**, W160-W165. doi:10.1093/nar/gkw257

Rapaport, D. H., Wong, L. L., Wood, E. D., Yasumura, D. and LaVail, M. M. (2004). Timing and topography of cell genesis in the rat retina. *J. Comp. Neurol.* **474**, 304-324. doi:10.1002/cne.20134

Read, K. A., Powell, M. D., Baker, C. E., Sreekumar, B. K., Ringel-Scaia, V. M., Bachus, H., Martin, R. E., Cooley, I. D., Allen, I. C., Ballesteros-Tato, A. et al. (2017). Integrated STAT3 and Ikaros zinc finger transcription factor activities regulate Bcl-6 expression in CD4(+) Th cells. *J. Immunol.* **199**, 2377-2387. doi:10.4049/jimmunol.1700106

Rhee, K.-D., Yu, J., Zhao, C. Y., Fan, G. and Yang, X.-J. (2012). Dnmt1-dependent DNA methylation is essential for photoreceptor terminal differentiation and retinal neuron survival. *Cell Death Dis.* **3**, e427. doi:10.1038/cddis.2012.165

Rieder, S. A., Metidji, A., Glass, D. D., Thornton, A. M., Ikeda, T., Morgan, B. A. and Shevach, E. M. (2015). Eos is redundant for regulatory T cell function but plays an important role in IL-2 and Th17 production by CD4+ conventional T cells. *J. Immunol.* **195**, 553-563. doi:10.4049/jimmunol.1500627

Roesch, K., Jadhav, A. P., Trimarchi, J. M., Stadler, M. B., Roska, B., Sun, B. B. and Cepko, C. L. (2008). The transcriptome of retinal Muller glial cells. *J. Comp. Neurol.* **509**, 225-238. doi:10.1002/cne.21730

Sagner, A. and Briscoe, J. (2019). Establishing neuronal diversity in the spinal cord: a time and a place. *Development* **146**, dev182154. doi:10.1242/dev.182154
Sapkota, D., Chintala, H., Wu, F., Fliesler, S. J., Hu, Z. and Mu, X. (2014). Onecut1 and Onecut2 redundantly regulate early retinal cell fates during development. *Proc. Natl. Acad. Sci. USA* **111**, E4086-E4095. doi:10.1073/pnas.1405354111
Schwickert, T. A., Tagoh, H., Gültekin, S., Dakic, A., Axelsson, E., Minnich, M., Ebert, A., Werner, B., Roth, M., Cimmino, L. et al. (2014). Stage-specific control of early B cell development by the transcription factor Ikaros. *Nat. Immunol.* **15**, 283-293. doi:10.1038/ni.2828
Sekiya, T., Kondo, T., Shichita, T., Morita, R., Ichinose, H. and Yoshimura, A. (2015). Suppression of Th2 and Tfh immune reactions by Nr4a receptors in mature T reg cells. *J. Exp. Med.* **212**, 1623-1640. doi:10.1084/jem.20142088
Sharma, M. D., Huang, L., Choi, J.-H., Lee, E.-J., Wilson, J. M., Lemos, H., Pan, F., Blazar, B. R., Pardoll, D. M., Mellor, A. L. et al. (2013). An inherently bifunctional subset of Foxp3+ T helper cells is controlled by the transcription factor eos. *Immunity* **38**, 998-1012. doi:10.1016/j.immuni.2013.01.013
Shimojo, H., Ohtsuka, T. and Kageyama, R. (2008). Oscillations in notch signaling regulate maintenance of neural progenitors. *Neuron* **58**, 52-64. doi:10.1016/j.neuron.2008.02.014
Skene, P. J., Henikoff, J. G. and Henikoff, S. (2018). Targeted in situ genome-wide profiling with high efficiency for low cell numbers. *Nat. Protoc.* **13**, 1006-1019. doi:10.1038/nprot.2018.015
Surzenko, N., Crowl, T., Bachleda, A., Langer, L. and Pevny, L. (2013). SOX2 maintains the quiescent progenitor cell state of postnatal retinal Muller glia. *Development (Cambridge, England)* **140**, 1445-1456. doi:10.1242/dev.071878
Taranova, O. V., Magness, S. T., Fagan, B. M., Wu, Y., Surzenko, N., Hutton, S. R. and Pevny, L. H. (2006). SOX2 is a dose-dependent regulator of retinal neural progenitor competence. *Genes Dev.* **20**, 1187-1202. doi:10.1101/gad.1407906
Turner, D. L., Snyder, E. Y. and Cepko, C. L. (1990). Lineage-independent determination of cell type in the embryonic mouse retina. *Neuron* **4**, 833-845. doi:10.1016/0896-6273(90)90136-4
Venkataraman, A., Yang, K., Irizarry, J., Mackiewicz, M., Mita, P., Kuang, Z., Xue, L., Ghosh, D., Liu, S., Ramos, P. et al. (2018). A toolbox of immunoprecipitation-grade monoclonal antibodies to human transcription factors. *Nat. Methods* **15**, 330-338. doi:10.1038/nmeth.4632
Wang, J.-H., Nichogiannopoulou, A., Wu, L., Sun, L., Sharpe, A. H., Bigby, M. and Georgopoulos, K. (1996). Selective defects in the development of the fetal and adult lymphoid system in mice with an Ikaros null mutation. *Immunity* **5**, 537-549. doi:10.1016/S1074-7613(00)80269-1
Wolf, F. A., Angerer, P. and Theis, F. J. (2018). SCANPY: large-scale single-cell gene expression data analysis. *Genome Biol.* **19**, 15. doi:10.1186/s13059-017-1382-0
Xiang, M. (1998). Requirement for Brn-3b in early differentiation of postmitotic retinal ganglion cell precursors. *Dev. Biol.* **197**, 155-169. doi:10.1006/dbio.1998.8868
Yang, Z., Ding, K., Pan, L., Deng, M. and Gan, L. (2003). Math5 determines the competence state of retinal ganglion cell progenitors. *Dev. Biol.* **264**, 240-254. doi:10.1016/j.ydbio.2003.08.005
Young, R. W. (1985a). Cell differentiation in the retina of the mouse. *Anat. Rec.* **212**, 199-205. doi:10.1002/ar.1092120215
Young, R. W. (1985b). Cell proliferation during postnatal development of the retina in the mouse. *Brain Res.* **353**, 229-239. doi:10.1016/0165-3806(85)90211-1
Yu, G., Wang, L.-G. and He, Q.-Y. (2015). ChIPseeker: an R/Bioconductor package for ChIP peak annotation, comparison and visualization. *Bioinformatics* **31**, 2382-2383. doi:10.1093/bioinformatics/btv145
Zheng, M.-H., Shi, M., Pei, Z., Gao, F., Han, H. and Ding, Y.-Q. (2009). The transcription factor RBP-J is essential for retinal cell differentiation and lamination. *Mol. Brain* **2**, 38. doi:10.1186/1756-6606-2-38
Zhu, M.-Y., Gasperowicz, M. and Chow, R. L. (2013). The expression of NOTCH2, HES1 and SOX9 during mouse retinal development. *Gene Expr. Patterns* **13**, 78-83. doi:10.1016/j.gep.2012.12.001
Zibetti, C., Liu, S., Wan, J., Qian, J. and Blackshaw, S. (2019). Epigenomic profiling of retinal progenitors reveals LHX2 is required for developmental regulation of open chromatin. *Commun. Biol.* **2**, 142. doi:10.1038/s42003-019-0375-9

Figure S1, Javed et al.

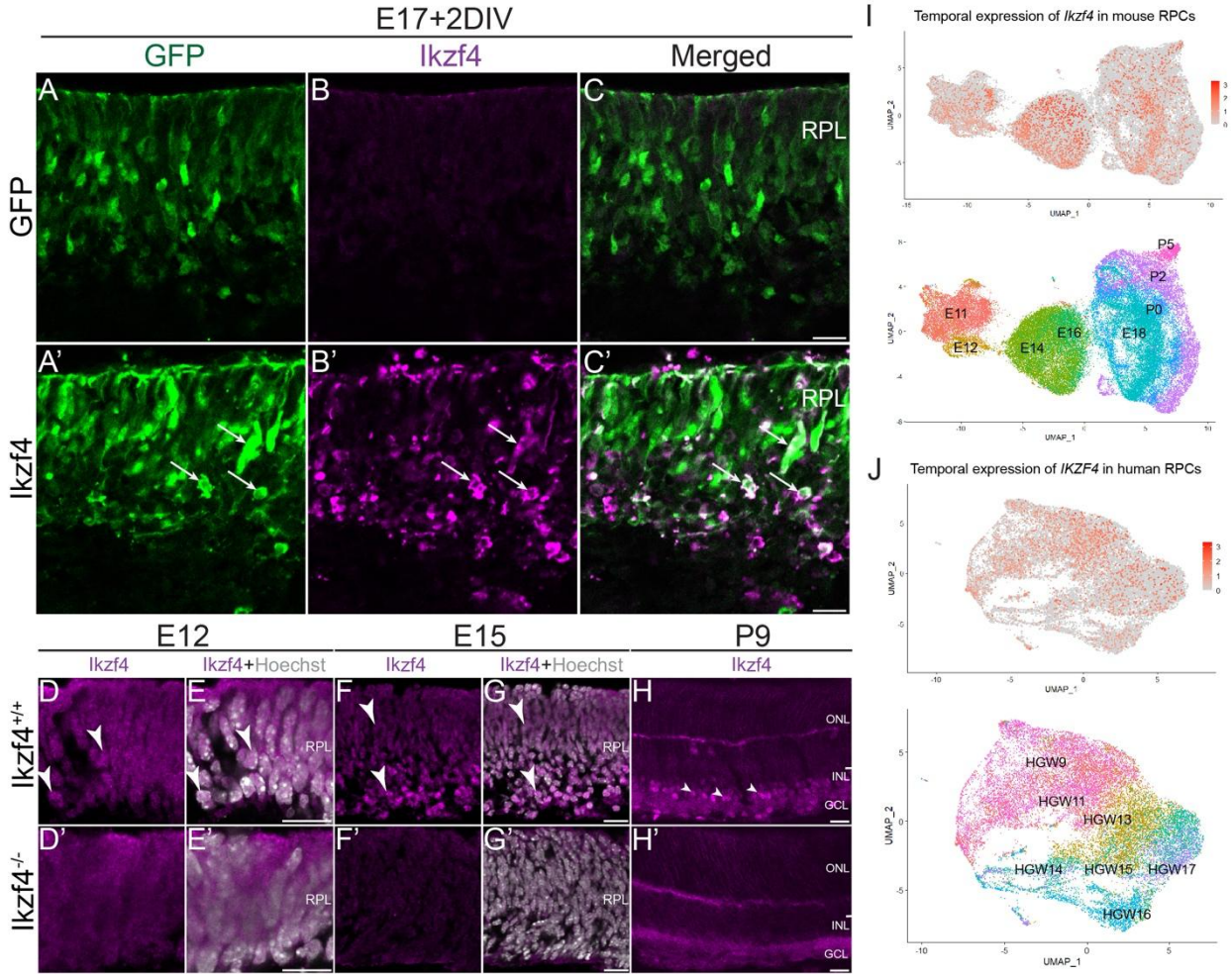

Fig. S1. Specificity of Ikzf4 antibody and scRNA-seq re-analysis of human and mouse RPCs.

(A-C') Examples of electroporation of either GFP (A-C) or Ikzf4-IRES-GFP (A'-C') in E17 retinas and immunostained with Ikzf4 antibody 2 days later. Note that these samples were fixed for 1 hour, which does not allow detection of endogenous Ikzf4 as reported in Figure 1 (fixed 2 mins). White arrows point to overexpressed Ikzf4, not endogenous. White arrows indicate $GFP^{+ve}Ikzf4^{+ve}$ cells. (D-H') Validation of the Ikzf4 antibody in $Ikzf4^{+/+}$ retinas (D-H) compared to $Ikzf4^{-/-}$ retinas (D'-H') at E12 (D-E'), E15 (F-G') and P9 (H-H'). White arrows show $Ikzf4^{+ve}$ cells with nuclear immunostaining. (I-J) Re-analysis of previously published single cell RNA-seq datasets from mouse (Clark et al. 2019) and human fetal (Lu et al. 2020) retinas. RPL: Retinal progenitor layer. ONL: Outer nuclear layer. INL: Inner nuclear layer. GCL: Ganglion cell layer. RPC: Retinal Progenitor Cell. HGW: Human Gestational Week. Scale bars: 10μm (A-H').

Figure S2, Javed et al.

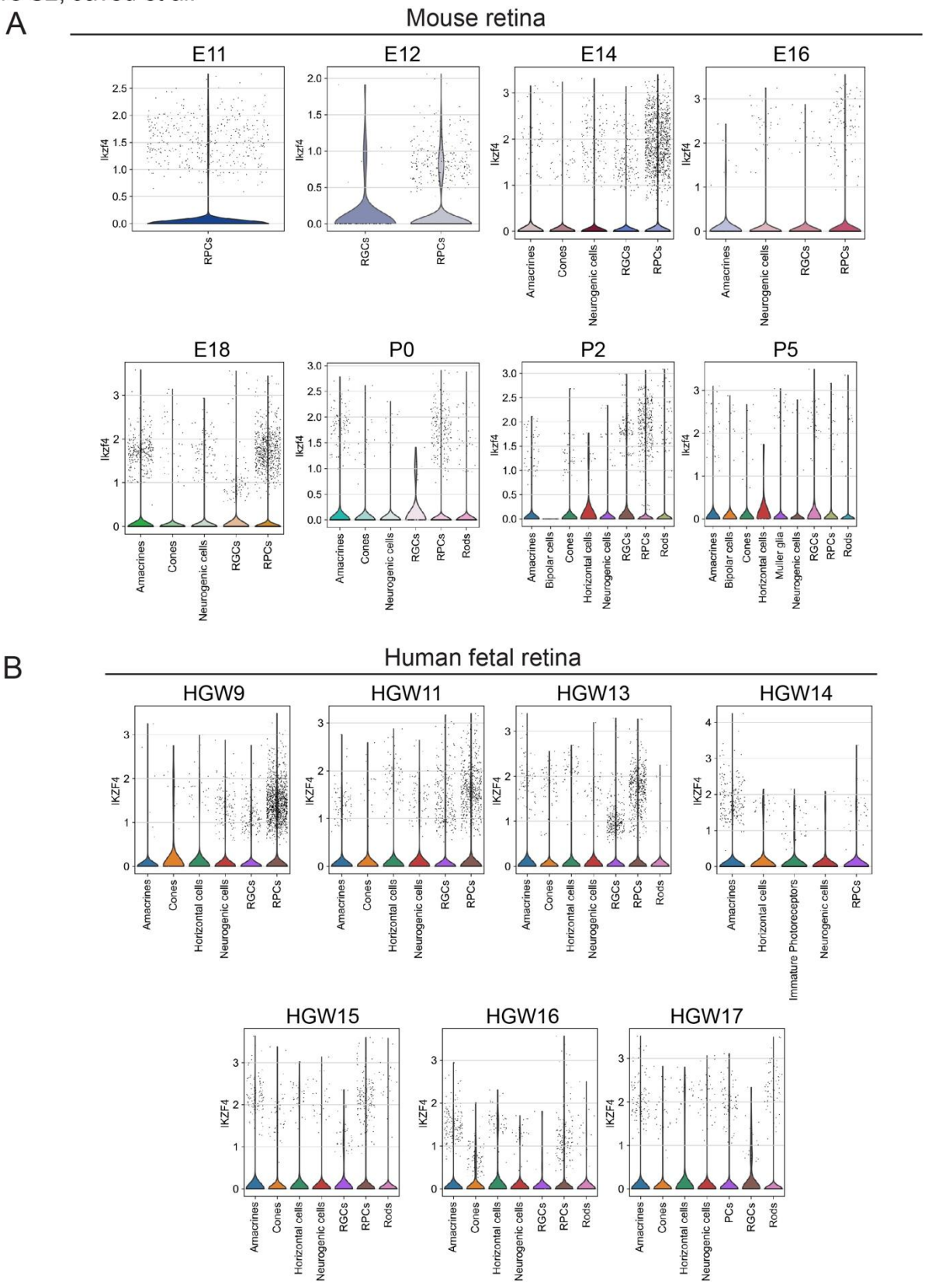

Fig. S2. *Ikzf4* mRNA is expressed in some differentiated cell types in mouse and human retina.

(A) Violin plot showing *Ikzf4* mRNA expression during mouse retinogenesis from previously published scRNA-seq dataset (Clark et al. 2019). (B) Violin plot showing *IKZF4* mRNA expression during early to late human fetal retinogenesis from previously published scRNA-seq dataset (Lu et al. 2020).

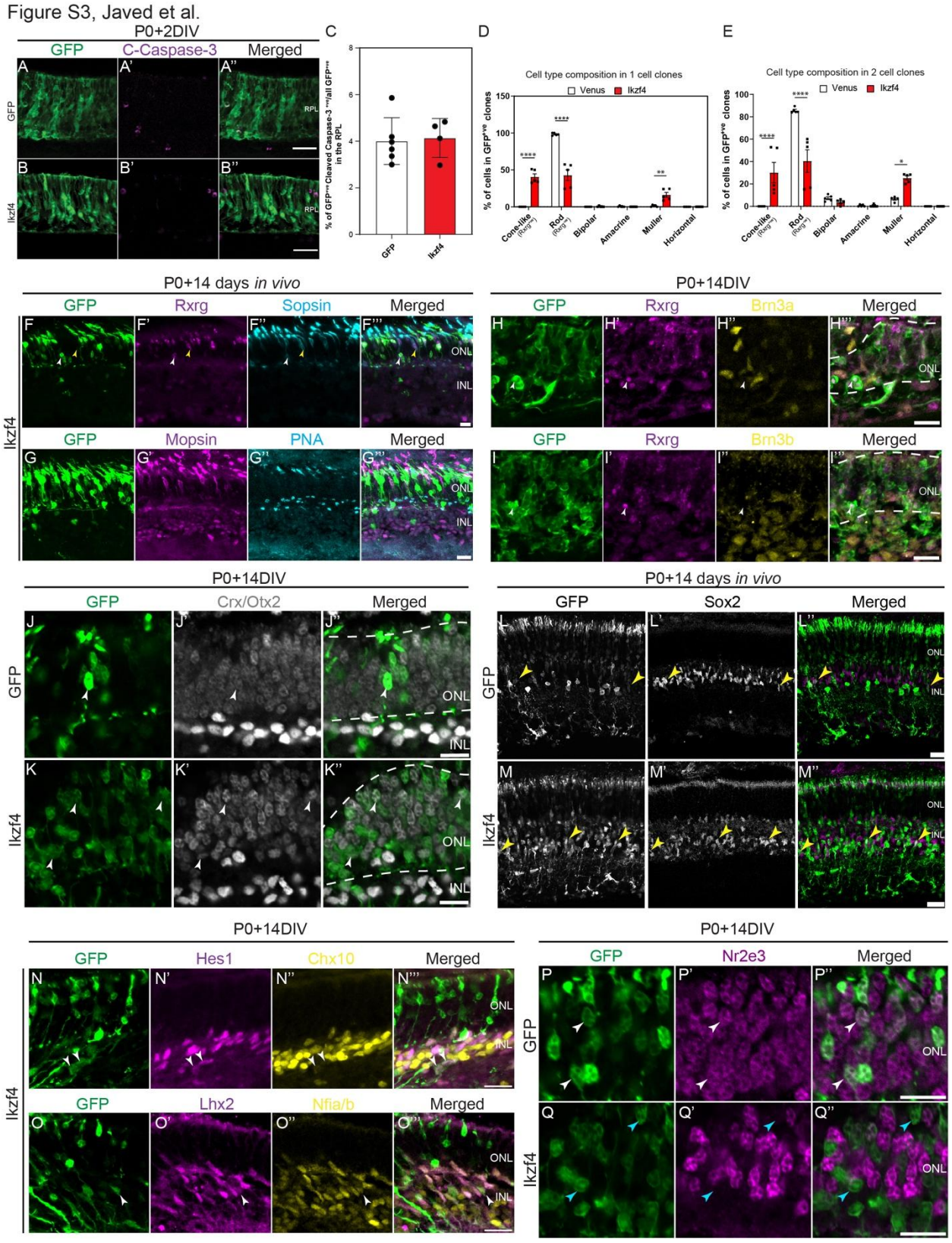

Fig. S3. Ikzf4 promotes cones and Müller glia from late RPCs by inducing early cell cycle exit rather than apoptosis.

(A-B') Examples of retinal explants electroporated at P0 with either GFP (A-B) or Ikzf4-IRES-GFP (A'-B') and immunostained with Cleaved Caspase-3 (B-B') 2 days later. (C) Quantification of GFP^{+ve} cells expressing Cleaved-Caspase-3 shown in (A-B'). (D-E) Retroviral clonal analysis of Venus or Ikzf4 as shown in (Fig. 2A-G) focusing on cell type composition of 1 cell (D) or 2 cell (E) clones. (F-G''') Examples of *in-vivo* electroporations at P0 with Ikzf4-IRES-GFP (F-G''') and immunostained 14 days later with Rxrg (F'), S-opsin (F''), M-opsin (G') or PNA (G''). White arrows denote $GFP^{+ve}Rxrg^{+ve}S\text{-}opsin^{-ve}$ cells whereas yellow arrow represent endogenous non-electroporated $Rxrg^{+ve}S\text{-}opsin^{+ve}$ cones. (H-I''') Examples of Ikzf4-IRES-GFP (H-I''') electroporations of retinal explants at P0 and co-immunostained 14 days later with Rxrg (H'-I') with either Brn3a (H'') or Brn3b (I''). (J-K'') Examples of retinal explants electroporated at P0 with either GFP (J-J'') or Ikzf4-IRES-GFP (K-K'') and immunostained with Crx/Otx2 (J-K') after 14 days of culture. Dashed lines highlight the outer nuclear layer. (L-M'') Examples of *in-vivo* electroporation of P0 retinas with either GFP (L-L'') or Ikzf4-IRES-GFP (M-M'') and immunostained with Sox2 (L'-M') 14 days later. (N-O''') Examples of retinal explants electroporated at P0 with Ikzf4-IRES-GFP (N-O''') and immunostained with Hes1 (N'), Chx10 (N''), Lhx2 (O') or Nfia/b (O''). White arrows represent either $Hes1^{+ve}Chx10^{-ve}$ cells (N-N''') or $Lhx2^{+ve}Nfia/b^{+ve}$ cells (O-O'''). (P-Q') Examples of retinal explants electroporated at P0 with either GFP (P-P'') or Ikzf4-IRES-GFP (Q-Q'') and immunostained with Nr2e3 (P'-Q') after 14 days of culture. White arrows represent $GFP^{+ve}Nr2e3^{+ve}$ cells whereas cyan arrows show $GFP^{+ve}Nr2e3^{-ve}$ cells. *p<0.05, **p<0.01, ****p<0.0001. Statistics: Two tailed unpaired t-test (D-E). ONL: Outer nuclear layer. INL: Inner nuclear layer. RPL: Retinal progenitor layer. Scale bars: 10μm (A-B', F-K'', N-Q''), 20μm (L-M'').

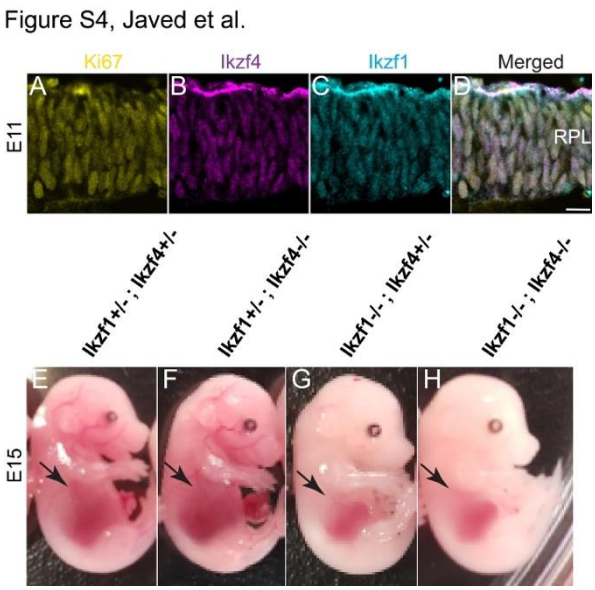

Fig. S4. Ikzf1 and Ikzf4 are expressed in the same cells during early retinogenesis and redundantly required for fetal liver size.

(A-D) Co-immunostaining of Ki67 (A), Ikzf4 (B), Ikzf1 (C) in E11 retinas. (E-H) Examples of E15 embryos with genotypes, $Ikzf1^{+/-}$;$Ikzf4^{+/-}$ (E), $Ikzf1^{+/-}$;$Ikzf4^{-/-}$ (F), $Ikzf1^{-/-}$;$Ikzf4^{+/-}$(G) or $Ikzf1^{-/-}$;$Ikzf4^{-/-}$ (H). Black arrows denote the fetal liver. RPL: Retinal progenitor layer. Scale bars: 10μm.

Figure S5, Javed et al.

A

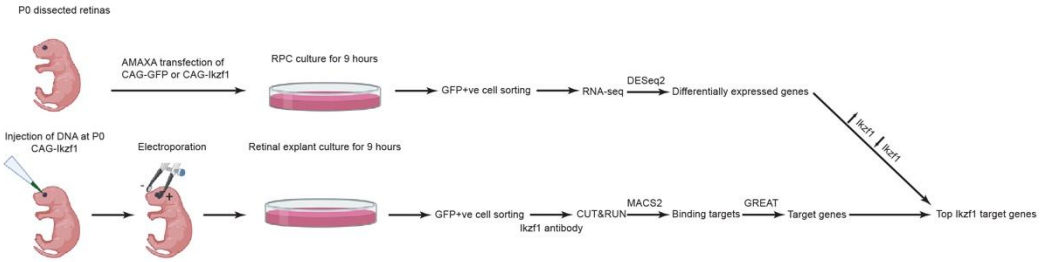

B

GO Biological process of upregulated genes in Ikzf1 RNA-seq

	GO_term_ID	GO_term_def	P	P_FDR_adj
1	GO:0007275	multicellular organism development	0.00E+00	1.00E-10
2	GO:0009966	regulation of signal transduction	0.00E+00	3.80E-09
3	GO:0048856	anatomical structure development	0.00E+00	1.00E-10
4	GO:0007399	nervous system development	0.00E+00	3.00E-10
5	GO:0048731	system development	0.00E+00	2.00E-10

Bhlhe22
Tfap2b
Nr4a2
Pax6

GO Biological process of downregulated genes in Ikzf1 RNA-seq

	GO_term_ID	GO_term_def	P	P_FDR_adj
1	GO:0007155	cell adhesion	0.00E+00	3.00E-10
2	GO:0007420	brain development	0.00E+00	2.20E-09
3	GO:0007154	cell communication	0.00E+00	2.00E-10
4	GO:0045664	regulation of neuron differentiation	0.00E+00	1.00E-10
5	GO:0032270	positive regulation of cellular protein metabolic process	0.00E+00	3.00E-10

Casz1
Hes1
Irx3
Rbpj
Sox2/9

C

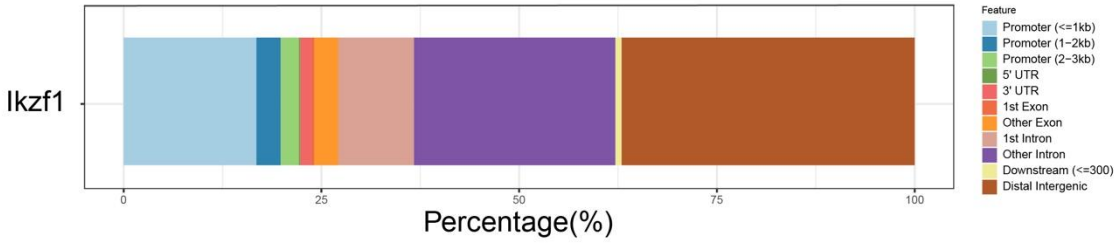

D

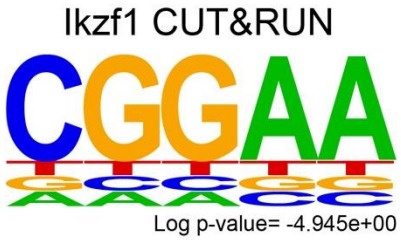

E

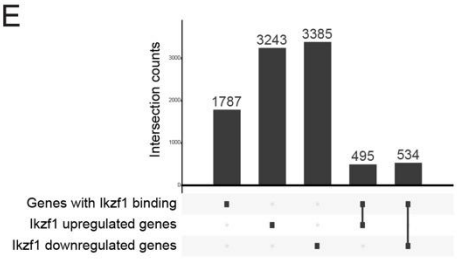

F

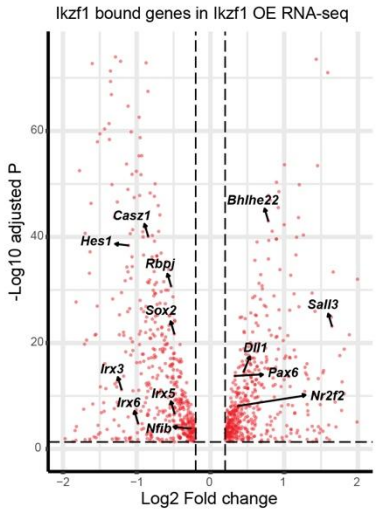

G

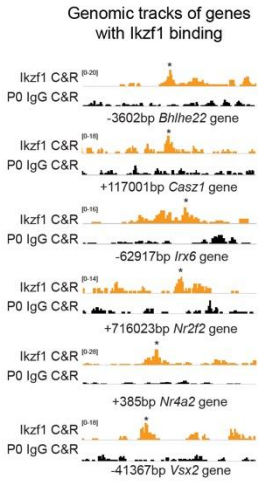

Fig. S5. Ikzf1 binds and upregulates early born cell type genes.

(A) Schematic showing the experimental design for Ikzf1 overexpression RNA-seq and CUT&RUN. (B) GONet analysis of top differentially regulated genes found in the RNA-seq dataset generated from Ikzf1 overexpressed RPCs. (C) ChIP-seeker genomic annotation of the Ikzf1 CUT&RUN peaks across the entire genome. (D) HOMER analysis showing canonical 'GGAA' motif enriched in Ikzf1 CUT&RUN peaks. (E) Upset plot representing the overlap between upregulated and downregulated genes from Ikzf1 overexpression RNA-seq and Ikzf1 CUT&RUN associated genes. (F) Volcano plot showing highlighted genes from (B) projected on the Ikzf1 RNA-seq data. (G) Genomic tracks of Ikzf1 CUT&RUN (orange) and P0 control IgG (black) on early and late genes found in (B). Asterisks indicate called peak.

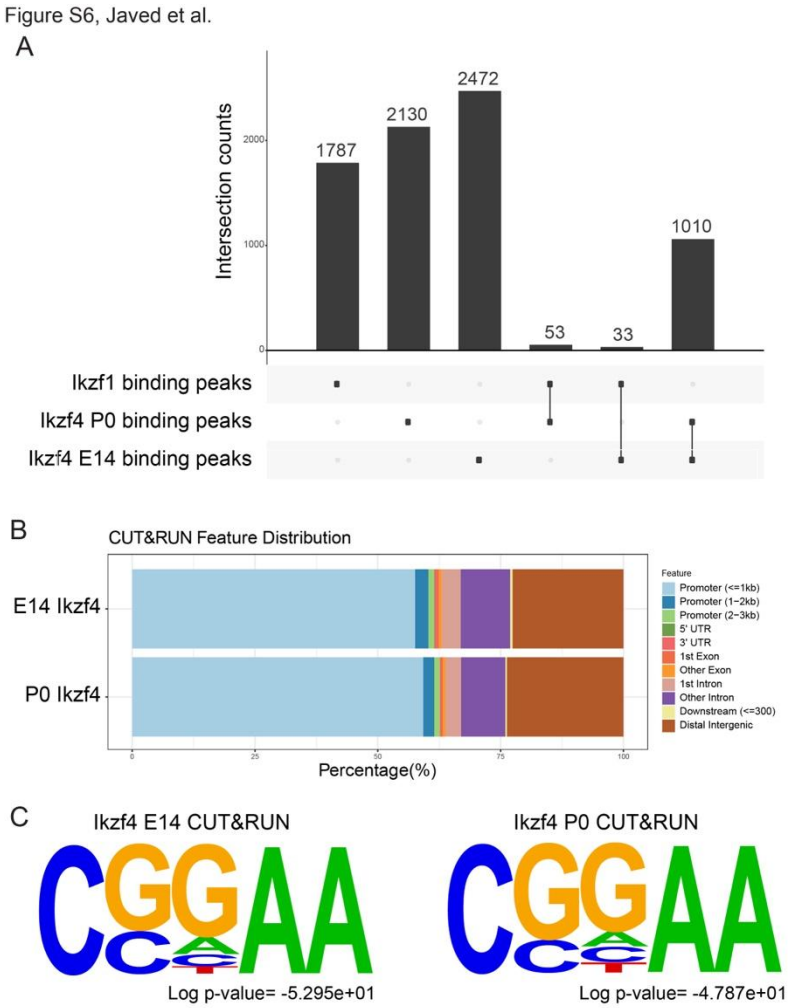

Fig. S6. Ikzf1 and Ikzf4 do not have a shared binding profile.

(A) Schematic showing the experimental design for Ikzf1 overexpression RNA-seq and CUT&RUN. (B) GONet analysis of top differentially regulated genes found in the RNA-seq dataset generated from Ikzf1 overexpressed RPCs. (C) ChIP-seeker genomic annotation of the Ikzf1 CUT&RUN peaks across the entire genome. (A) Upset plot representing the overlap between Ikzf1 CUT&RUN peaks and Ikzf4 CUT&RUN E14/P0 peaks. (B) ChIP-seeker genomic annotation of the Ikzf4 CUT&RUN E14/P0 peaks across the entire genome. (C) HOMER analysis showing canonical 'GGAA' motif enriched in Ikzf4 CUT&RUN E14/P0 peaks.

Figure S7, Javed et al.

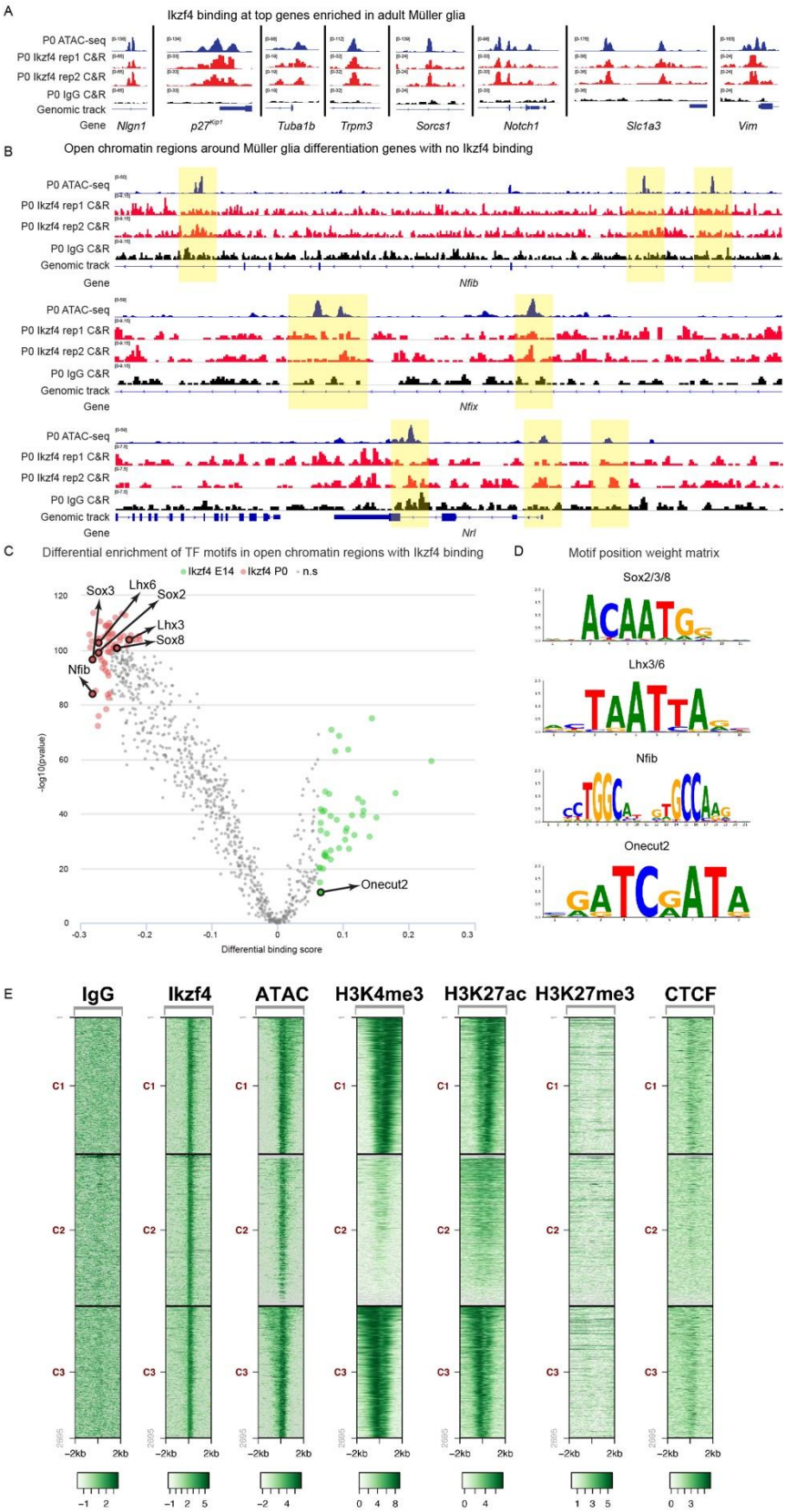

Fig. S7. Ikzf4 binds to cis regulatory regions important for Müller glia differentiation. (A) Genomic tracks of ATAC-seq at P0 in blue (Aldiri et al. 2017), two replicates of Ikzf4 CUT&RUN at P0 in red, or IgG Control CUT&RUN at P0 in black at genomic location of Müller glia genes enriched in scRNA-seq dataset of P14 mouse retinas (Clark et al. 2019). (B) Genomic tracks of ATAC-seq at P0 in blue (Aldiri et al. 2017), two replicates of Ikzf4 CUT&RUN at P0 in red, or IgG Control CUT&RUN at P0 in black at genomic location of *Nfib*, *Nfix* and *Nrl*. Yellow highlighted areas indicate regions with positive ATAC-seq signal but negative Ikzf4 CUT&RUN signal. (C) Volcano plot of TOBIAS BINDetect TF footprinting analysis on open chromatin regions bound by Ikzf4 at E14 and P0. Arrows indicate motif with TF name. (D) Representative motif position weight matrix for TFs listed in (C). (E) Seqplot heatmaps of P0 IgG C&R, P0 Ikzf4 C&R, ATAC-seq, H3K4me3, H3K27ac, H3K27me3 and CTCF ChIP-seq from (Aldiri et al. 2017). TF: Transcription factor.

Figure S8, Javed et al.

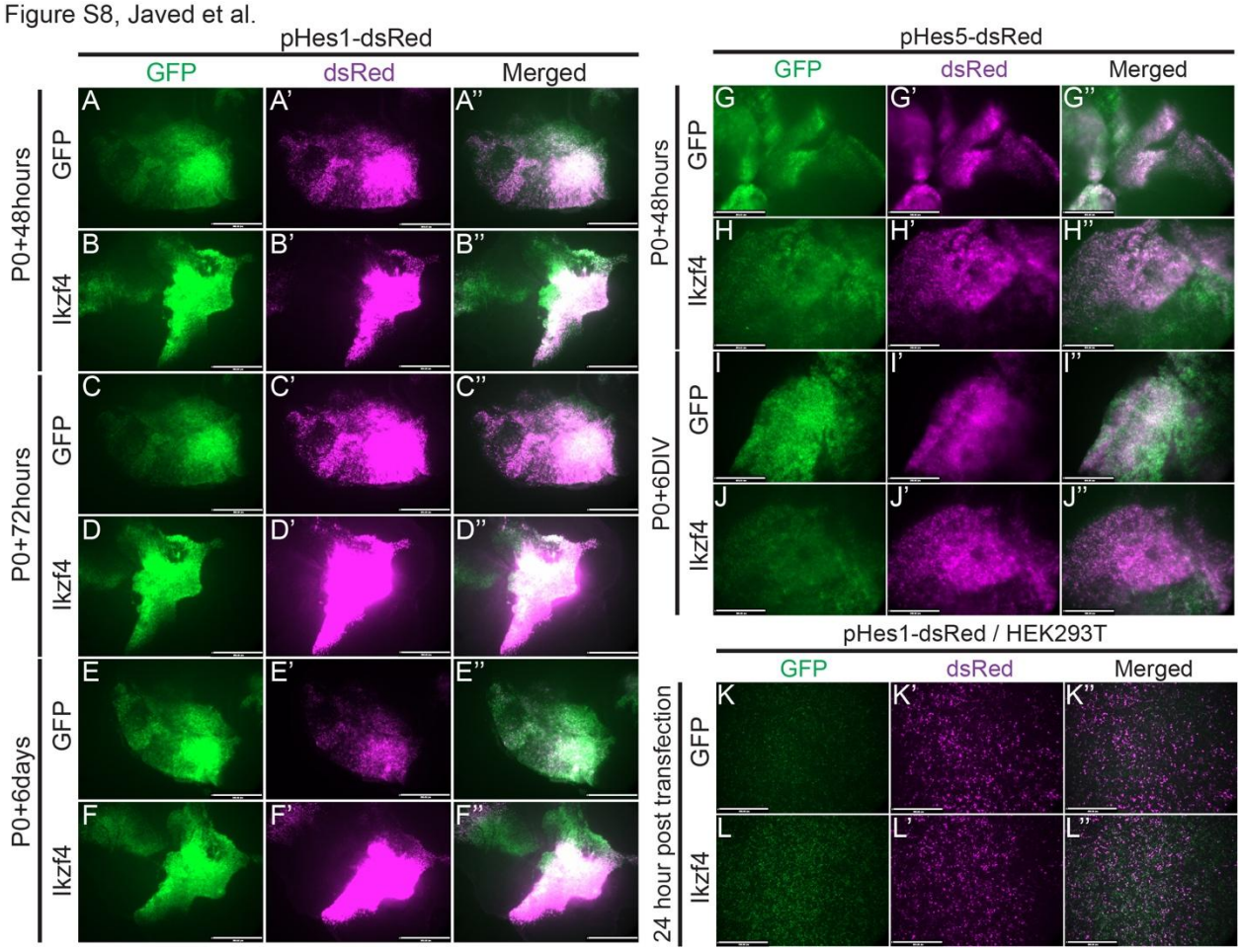

Fig. S8. Ikzf4 maintains Hes1 expression in post-mitotic cells during late retinogenesis. (A-J'') Photomicrographs of retinal explants co-electroporated at P0 with Hes1-dsRed or Hes5-dsRed and either GFP (A-A'', C-C'', E-E'', G-G'', I-I'') or Ikzf4-IRES-GFP (B-B'', D-D'', F-F'', H-H'', J-J'') followed by imaging after either 48hours (A-B'', G-H''), 72hours (C-D''), or 6 days (E-F'', I-J''). (K-L'') Photomicrographs of HEK293T cells transfected with Hes1-dsRed and either GFP (K-K'') or Ikzf4-IRES-GFP (L-L'') imaged 24hours post-transfection. Scale bars: 360μm (A-L'').

Table S1. CSV file containing differentially expressed genes between P0+9hours RPC expressed CAG-GFP or CAG-Ikzf4-IRES-GFP.

Click here to download Table S1

Table S2. CSV file containing GONet analysis of Ikzf1 upregulated genes in P0+9hours RPCs.

Click here to download Table S2

Table S3. CSV file containing GONet analysis of Ikzf1 downregulated genes in P0+9hours RPCs.

Click here to download Table S3

Table S4. TXT file showing GREAT analysis of Ikzf1 P0+9hours CUT&RUN gene and peak location.

Click here to download Table S4

Table S5. CSV file containing differentially expressed genes between P0+9hours RPC expressed CAG-GFP or CAG-Ikzf4-IRES-GFP also associated with Ikzf1 binding.

Click here to download Table S5

Table S6. TXT file showing GREAT analysis of Ikzf4 E14 binding target gene and peak location.

Click here to download Table S6

Table S7. TXT file showing GREAT analysis of Ikzf4 P0 binding target gene and peak location.

Click here to download Table S7

Table S8. Excel spreadsheet containing the complete list of differential enriched motifs between Ikzf4 E14 and Ikzf4 P0 open chromatin regions using TOBIAS BINDetect.

Click here to download Table S8

Table S9: Sequences of primers

Click here to download Table S9

Table S10. Materials

Click here to download Table S10